Hypothalamic hormone deficiency enables physiological anorexia

Sarah M. Mohr[1,2,3], Rafael Dai Pra[1,2,3], Maryann P. Platt[1,2,3], Viktor V. Feketa[1,2,3], Marya Shanabrough[4], Luis Varela[4,5], Ashley Kristant[4], Haoran Cao [1,2,3], Dana K. Merriman[6], Tamas L. Horvath[4,5], Sviatoslav N. Bagriantsev[1*], and Elena O. Gracheva[1,2,3*]

[1]Department of Cellular and Molecular Physiology, Yale University School of Medicine, 333 Cedar Street, New Haven, CT 06510, USA

[2]Department of Neuroscience, Yale University School of Medicine, 333 Cedar Street, New Haven, CT 06510, USA

[3]Kavli Institute for Neuroscience, Yale University School of Medicine, 333 Cedar Street, New Haven, CT 06510, USA

[4]Department of Comparative Medicine, Yale University School of Medicine, 310 Cedar Street, New Haven, CT 06510, USA.

[5]Achucarro Basque Center for Neuroscience, Leioa, Spain 48940

[6]Department of Biology, University of Wisconsin-Oshkosh, 800 Algoma Boulevard, Oshkosh, WI 54901, USA

*Correspondence: slav.bagriantsev@yale.edu and elena.gracheva@yale.edu

Abstract

Mammalian hibernators survive prolonged periods of cold and resource scarcity by temporarily modulating normal physiological functions, but the mechanisms underlying these adaptations are poorly understood. The hibernation cycle of thirteen-lined ground squirrels *(Ictidomys tridecemlineatus)* lasts for 5–7 months and comprises weeks of hypometabolic, hypothermic torpor interspersed with 24–48-hour periods of an active-like interbout arousal (IBA) state. We show that ground squirrels, who endure the entire hibernation season without food, have negligible hunger during IBAs. These squirrels exhibit reversible inhibition of the hypothalamic feeding center, such that hypothalamic arcuate nucleus neurons exhibit reduced sensitivity to the orexigenic and anorexigenic effects of ghrelin and leptin, respectively. However, hypothalamic infusion of thyroid hormone during an IBA is sufficient to rescue hibernation anorexia. Our results reveal that thyroid hormone deficiency underlies hibernation anorexia and demonstrate the functional flexibility of the hypothalamic feeding center.

Introduction

In humans, inhibition of food intake, or anorexia, can manifest as a serious disorder that impacts quality of life and in severe cases can cause death. Anorexia can describe the lack of hunger due to pathological conditions, for example during cancer cachexia, or in the psychiatric condition anorexia nervosa, in which subjects self-limit eating despite a negative energy balance. Physiological anorexia is observed in toddlers and elderly adults who, during certain developmental periods, become less interested in food and reduce their food intake. The mechanisms underlying various types of anorexia remain poorly understood, though recent evidence strongly suggests that, in addition to psychological and social factors, anorexia is driven by physiological changes[1–6].

For thirteen-lined ground squirrels (*Ictidomys tridecemlineatus,* Fig. 1a), who do not rely on stored food during hibernation, anorexia is an essential component of a normal physiological cycle. Because premature emergence from the safety of the underground burrow to search for food would defeat the purpose of hibernation and pose a risk of predation, anorexia constitutes an important safety mechanism that increases survival.

A seasonal cycle of ground squirrels consists of several physiological states. In the active state (late spring to late summer), squirrels are euthermic, hyperphagic and metabolically active. During the pre-hibernation state (late summer to early fall), squirrels reduce food consumption and undergo temporary bouts of hypothermia. Hibernation (early fall to late spring) consists of repeated cycles of hypothermic torpor interspersed with brief periods of euthermic IBA. During torpor, animals enter a state of suspended animation by profoundly reducing their metabolic, heart and respiration rates, and lowering their body temperature to 2–4 °C. Every 2–3 weeks, squirrels arouse to spend ~24 hours in IBA (Fig. 1b), when their main bodily functions temporarily return to an active-like state[7]. Ground squirrels do not depend on stored food during hibernation; instead, energy is supplied by body fat amassed during the summer. Thus, although hibernating squirrels resemble fasted animals metabolically, they demonstrate little interest in food despite enduring over seven months of starvation[8–11]. We sought to understand the mechanism underlying this remarkable example of reversible anorexia by comparing euthermic animals during the active season with euthermic animals during IBAs in the hibernation season. Our

experiments reveal that hibernation anorexia is caused by thyroid hormone deficiency in the hypothalamus.

Results

Hibernating ground squirrels exhibit negligible food consumption

We found that when squirrels were presented with food during the numerous IBAs throughout the hibernation season, they consumed approximately six times less food than during the active state, and 3 times less than during the pre-hibernation state (Active: 14.0 ± 0.8 g/day, pre-hibernation: 7.6 ± 0.7 g/day, IBA: 2.4 ± 0.2 g/day; One-Way ANOVA with Dunnett's multiple comparison test: Active vs Pre-hibernation, $P < 0.0001$; IBA vs Active, $P < 0.0001$; IBA vs Pre-hibernation, $P < 0.001$; Fig. 1c and Extended Data Fig. 1). Their body weight continuously decreased throughout hibernation, reaching ~50% of their starting weight by the end of the season (Fig. 1c and Extended Data Fig. 1). Concurrently with body weight reduction, IBA squirrels progressively reduced serum levels of glucose (Active: 22.2 ± 2.9 mM, IBA: 12.8 ± 1.1 mM; Mann-Whitney test, $P < 0.001$) and insulin (Active: 44.4 ± 7.4 µU/mL, IBA: 8.4 ± 1.3 µU/mL; student's t-test, $P < 0.0001$; Fig. 1d, e and Extended Data Fig. 1). Consistent with the idea that fat becomes the primary energy source during hibernation, IBA squirrels exhibited increased levels of serum β-hydroxybutyrate (Active: 0.23 ± 0.04 mM, IBA: 2.07 ± 0.25 mM; student's t-test, $P < 0.0001$; Fig. 1f). Thus, despite many months of fasting and extensive utilization of internal fat resources, hibernating squirrels exhibit negligible food consumption (anorexia).

Hibernating squirrels demonstrate reversible resistance to ghrelin

During fasting, the stomach releases the orexigenic hormone ghrelin, which activates Agouti-Related Peptide/Neuropeptide Y (AgRP/NPY) neurons in the arcuate nucleus of the hypothalamus (ARC), stimulating food consumption[12–16]. We tested whether anorexia during hibernation is caused by low levels of ghrelin. However, we found no significant difference in total and acylated (active) forms of ghrelin in blood plasma between IBA and active squirrels; instead, acylated ghrelin showed a trend towards increasing during hibernation (Fig. 2a–c). Because the high ghrelin levels observed during IBA are sufficient to induce feeding in active animals, we hypothesized that hibernating squirrels develop seasonal ghrelin resistance[8,17]. We tested this by monitoring food consumption in active and IBA squirrels after peripheral injection

88 of ghrelin. As expected, ghrelin potentiated feeding in active squirrels to levels observed in mice
89 and rats[18–20], and exceeding those of active squirrels after 48 hours of food deprivation (Active
90 PBS: 0.3 ± 0.2 g, Active Ghrelin: 2.3 ± 0.3 g; Two-Way ANOVA with Tukey's post hoc test, Active
91 PBS v Active Ghrelin, $P < 0.001$; Fig. 2d, e). In stark contrast, ghrelin failed to potentiate food
92 consumption when injected during IBAs, suggesting ghrelin resistance (IBA PBS: 0.2 ± 0.1 g, IBA
93 Ghrelin: 0.4 ± 0.1 g; Two-Way ANOVA with Tukey's post hoc test, $P = 0.14$; Fig. 2d). To further
94 challenge this conclusion, we compared the effect of ghrelin injection in IBA animals during
95 hibernation and in the same animals after they became active after hibernation arousal. Active
96 animals showed almost six-fold elevated food consumption compared to when they were in IBA,
97 further strengthening the notion of ghrelin resistance during IBA (IBA ghrelin: 0.4 ± 0.1 g, Active
98 ghrelin: 2.5 ± 0.3 g; paired student's t-test, $P < 0.02$; Fig. 2f).

99 Immunohistochemical analysis of *cFOS* expression showed that ghrelin injections
100 activated a subset of ARC neurons in active, but not IBA, animals (Fig. 2g–i), suggesting that ARC
101 neurons have reduced sensitivity to ghrelin during hibernation. In normal physiological
102 conditions, ghrelin binds to growth-hormone secretagogue receptors (*Ghsr*) on AgRP/NPY
103 neurons, triggering a release of the AgRP peptide from nerve terminals. Therefore, AgRP is
104 predominantly found in nerve terminals rather than neuronal soma[13,21–25], a pattern we observed
105 in active animals (Fig. 2j). In contrast, and in agreement with the idea of diminished sensitivity to
106 ghrelin during IBA, AgRP accumulated in neuronal somas of IBA animals (Active: 0.8 ± 0.5, IBA:
107 47.4 ± 4.9 cell bodies, Mann-Whitney test, $P < 0.0001$ Fig. 2j, k and Extended Data Fig. 2), implying
108 a diminished release of the peptide from these neurons.

109 **Hibernating squirrels have reduced leptin signaling**

110 To investigate whether additional mechanisms contribute to hibernation anorexia, we
111 asked if ARC neurons are sensitive to the satiety hormone leptin during IBAs. We found that
112 plasma levels of leptin were slightly elevated in IBAs compared to active animals (Fig. 3a).
113 However, during IBA ARC neurons showed reduced levels of the phosphorylated form of the
114 signal transducer and activator of transcription 3 (pSTAT3) – a marker for leptin signaling in
115 neurons[26] (Fig. 3b, c). Furthermore, we observed a decrease in the abundance of pSTAT3+ cells
116 expressing *cFOS* (Fig. 3b-e). A subset of leptin-responsive neurons is marked by the expression of

117 pro-opiomelanocortin (POMC) peptide and is responsible for producing satiety[27,28]. We observed
118 a reduction in the abundance of POMC+ and POMC+/cFOS+ neurons during IBA, suggesting
119 reduced activity in these cells (Fig. 3f–i). Together, these data show that leptin signaling in ARC
120 neurons is reduced in hibernating squirrels.

121 **Ghrelin and leptin receptors and BBB funtion are unaltered during hibernation**

122 To understand the mechanism for reduced ghrelin and leptin signaling during hibernation,
123 we performed single cell sequencing of arcuate nucleus and median eminence (ARC-ME) neurons
124 from active and IBA squirrels. 88,304 cells from ARC-ME were captured and analyzed after quality
125 control (Active: 48,920 cells from 3 animals; IBA: 39,384 cells from 3 animals). ARC-ME tissue
126 from squirrels in both states contained major cell types expected to be present in this brain area
127 (Fig. 5a). Further sub-clustering of neurons identified major neuronal populations, similar to
128 those found in the ARC of mice[23], including *Pomc/Cartpt*, *Agrp/Npy*, *Kiss, Ghrh*, *Sst*, and *Th*-
129 expressing subclusters (Fig. 4a, c and Extended Data Table 1). AgRP and POMC neuronal clusters
130 expressed known markers of these populations, confirming their identity[29] (Fig. 4b).

131 Based on our single-cell dataset, we found that the levels of ghrelin receptors in AgRP
132 neurons and leptin receptors in POMC neurons remained unchanged between active and IBA
133 animals (Fig. 4d, f). Furthermore, over 95% of *Ghsr* and over 89% of *Lepr* transcripts cloned *de*
134 *novo* from the ARC represented functional isoforms[24,30] (Fig. 4e, g). Next, we tested whether
135 blood brain barrier (BBB) function was impaired during hibernation, which would reduce
136 peripheral hormone transport to the brain. Injections of 3 kDa dextran and 860 Da biocytin into
137 active and IBA animals showed that ARC BBB retained its integrity during hibernation (Fig. 4h–j
138 and Extended Data Fig. 3). Thus, the reduced ghrelin and leptin signaling in the ARC cannot be
139 entirely attributed to a lack of functional receptors or impaired BBB, suggesting other
140 mechanisms.

141 **Hibernating animals demonstrate central hypothyroidism**

142 Our findings that ARC neurons resist the orexigenic effects of ghrelin and exhibit reduced
143 leptin signaling during IBA suggested that activity of the hypothalamic feeding center is
144 temporarily suppressed during hibernation. To understand the mechanism of this suppression,
145 we turned our attention to the thyroid hormone triiodothyronine (T3), which stimulates food

146 intake by acting on hypothalamic nuclei[31–35]. It has further been shown that the excitability of
147 ARC AgRP neurons during fasting or ghrelin administration is increased by central thyroid
148 hormone via uncoupling protein 2 (UCP2)-dependent mitochondrial proliferation[36,37]. We
149 therefore hypothesized that anorexia during IBA may be due to central T3 deficiency.

150 The translocation of T3 and its precursor T4 from the circulation to neurons occurs, in
151 part, via the monocarboxylate transporter 8 (MCT8) expressed in endothelial cells and
152 tanycytes[38–40]. Accordingly, our single cell RNA sequencing revealed MCT8 expression in these
153 cell types in squirrel ARC (Fig. 5a). Furthermore, during IBA we observed a significant decrease in
154 *MCT8* expression in tanycytes, but not in neurons or endothelial cells (Fig. 5b–h). Next, we
155 assessed the level of expression of the immunoglobulin superfamily member 1 (*Igsf1*). Loss of
156 function mutations in IGSF1 causes central hypothyroidism in humans and mice[41–45]. *Igsf1* was
157 expressed in neurons and astrocytes of squirrel ARC, and the level of expression significantly
158 decreased in both groups during IBA (Extended Data Fig. 4). These results suggest a potential
159 decrease in hypothalamic T3 during hibernation. In support of this, direct measurements showed
160 more than two-fold lower levels of hypothalamic T3 during IBA compared to active animals
161 (Active: 0.77 ± 0.1 pg/mg tissue, IBA: 0.32 ± 0.05 pg/mg tissue; student's t-test, $P < 0.01$; Fig. 6a).
162 We also detected a steady decline in hypothalamic T3 during the active season, reaching the level
163 observed during IBA by the end of hibernation (Fig. 6a). At the same time, the level of T3 in blood
164 serum remained unchanged, demonstrating that thyroid hormone deficiency during hibernation
165 was restricted to the CNS (Fig. 6b). We also found significantly higher blood serum levels of T4
166 during IBA (Fig. 6c), further supporting the idea that hibernating squirrels exhibit central, but not
167 peripheral, hypothyroidism.

168 Thyroid hormones canonically exert their action by binding to nuclear thyroid hormone
169 receptors alpha (*Thra*) and beta (*Thrb*)[46]. Single-cell sequencing of ARC neurons revealed that
170 *Thra* and *Thrb* are expressed in AgRP and POMC neurons , and that their expression levels are
171 similar in both physiological states (Fig. 6d, e), suggesting that hypothyroidism in IBA animals is
172 not caused by receptor downregulation.

173 **Central T3 infusion rescues hibernation anorexia**

174 Our data suggest that anorexia during hibernation is caused by hypothalamic T3
175 deficiency. To test this hypothesis, we bypassed this transport step by infusing T3 directly into
176 the mediobasal hypothalamus during IBA and measured its effect on feeding (Fig. 6f).
177 Remarkably, while T3 injection did not induce feeding during the first two hours post-injection
178 (Fig. 6g,h, left), it resulted in robust and significant potentiation of feeding over a 24-hour period
179 (Hibernation Season 1: Control: 1.6 ± 0.3 g, 15.3 nmol T3: 2.5 ± 0.3; paired student's t-test, $P <$
180 0.001; Hibernation Season 2: Control: 1.6 ± 0.6 g, 15.3 pmol T3: 3.3 ± 0.9 g; paired student's t-
181 test, $P = 0.02$; Fig. 6g,h, right), consistent with its role as a transcriptional regulator. Thus, these
182 data show that the specific deficiency of T3 in the CNS contributes to reversible anorexia during
183 hibernation.

184 **Discussion**

185 Hibernation was first documented in 350 BCE by Aristotle, who noted that some creatures
186 cease eating and conceal themselves in a sleep-like state for many months to pass the winter[47].
187 Hibernation invokes a series of flexible adaptations that allow animals to thrive in inhospitable
188 environments, where they experience thermal challenges and food scarcity[48]. Coordination of
189 hunger and satiety is essential for hibernators to survive, as premature emergence from
190 underground burrows to seek food may dysregulate dependent processes and increase the risk
191 of predation. In this study, we found that squirrels exhibit T3 deficiency in the hypothalamus
192 during IBA and that restoration of T3 in the hypothalamus reverses anorexia, demonstrating that
193 long-term suppression of hunger during hibernation is, at least partially, due to central
194 hypothyroidism.

195 Our findings demonstrate that thyroid hormone deficiency during hibernation is
196 restricted to the CNS and does not extend to peripheral levels of T3 and T4. Hibernating squirrels
197 thus present a remarkable animal model in which central thyroid hormone function is depressed
198 while essential peripheral thyroid function on internal organs and general metabolic processes is
199 preserved[49,50]. Central thyroid hormone has been implicated in the seasonal shifts in
200 reproduction and food intake in non-hibernating animals, including Siberian hamsters, sheep,
201 photoperiodic F344 rats[51–54]and hibernating arctic ground squirrels[55].

202 Although the precise mechanism of central hypothyroidism remains to be determined in our
203 model, the data presented here suggest a putative mechanism with two complimentary steps.
204 The first step involves a reduction in MCT8 expression, leading to limited transport of thyroid
205 hormone from circulation into the hypothalamus. This finding echoes data in humans and mice,
206 where loss of functional MCT8 leads to central hypothyroidism, causing a panel of metabolic and
207 neurological abnormalities[56–58]. The second step involves IGSF1, a protein expressed in squirrel
208 hypothalamic neurons and astrocytes. IGSF1 dysfunction is strongly linked with congenital
209 central hypothyroidism in humans, and this phenotype is recapitulated in mouse models[41–45].
210 Although the exact mechanism of IGSF1 is a matter of intense research, our data suggest that
211 reversible IGSF1 deficiency in hypothalamic neurons could be part of the natural seasonal
212 physiology of squirrels, contributing to reversible anorexia during hibernation. Our data show
213 that, in contrast to humans, central hypothyroidism in squirrels is an essential component of
214 normal physiology. In both cases, however, this process relies on similar molecular pathways,
215 suggesting hibernating squirrels as a naturalistic model to study the mechanism of central
216 hypothyroidism and associated diseases in humans.

Acknowledgements. We thank Lyle Murphy for technical assistance, and members of the Gracheva and Bagriantsev laboratories for comments and critique throughout the study. We thank Dr. Rachel Perry for performing the Leptin ELISA.

Funding. This work was funded by a Gruber Foundation Fellowship (SMM), The Kavli Foundation (MPP), National Institutes of Health grants R01NS097547 (SNB), and National Science Foundation grants 1923127 (SNB) and 1754286 (EOG). RDP was supported by a scholarship from Coordenação de Aperfeiçoamento de Pessoal de Nível Superior (CAPES), Brazil.

Author contributions. Conceptualization: SMM, EOG, SNB. Data collection: SMM, RDP, MPP, VF, MS, LV, AK, HC, TLH. DKM supplied squirrels and provided advice on animal husbandry. Funding acquisition, project administration and supervision: EOG and SNB. Writing: SMM, RDP, EOG, SNB, TLH with contribution from DKM, MPP, HC.

Competing Interests. Authors declare that they have no competing interests.

Data and materials availability. All data are available in the main text or the supplementary materials. The RNA sequencing data was deposited to the Gene Expression Omnibus, accession number: GSE242381.

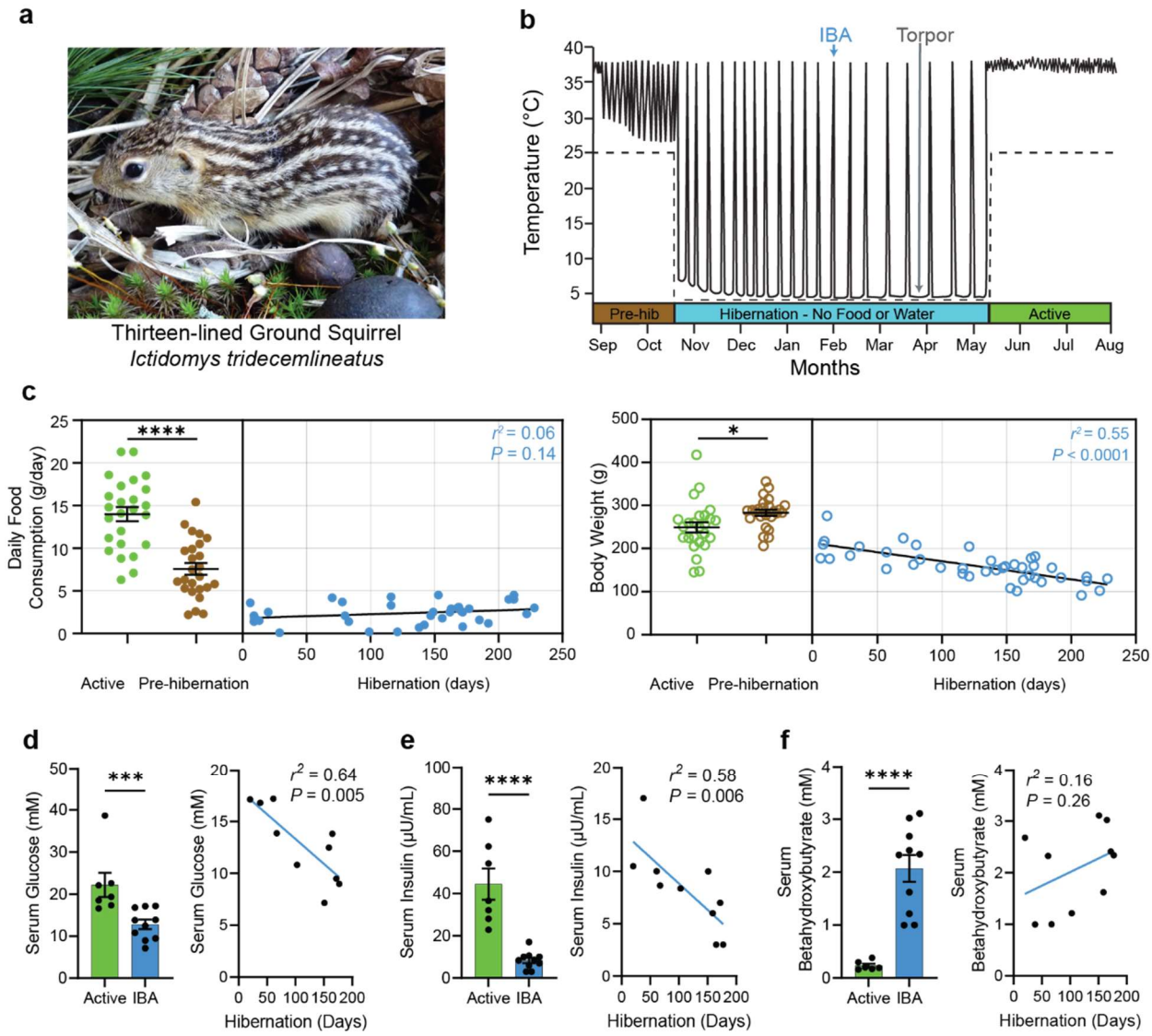

Fig. 1. Hibernating ground squirrels exhibit negligible food consumption.
a, Image of a thirteen-lined ground squirrel, *Ictidomys tridecemlineatus.*
b, Schematic of ground squirrel core body temperature before, during and after hibernation. Dotted line, ambient temperature. Every temperature peak during hibernation represents an IBA. *IBA*: interbout arousal *Pre-hib*: Pre-hibernation.
c, Daily food consumption (left) and body weight (right) during the active (summer), pre-hibernation (fall), and hibernation (winter) season. Active feeding data is peak summer food consumption. Pre-hibernation feeding data is the last daily feeding measurement that the animal maintains euthermia (mean ± SEM, n = 25 Active animals, student's t-test, $P < 0.0001$; n = 25 Pre-hibernation animals, student's t-test, $P < 0.05$). Hibernation feeding and body weight was measured during IBAs and is plotted by days in hibernation. (n = 35 animals for food consumption and n = 42 animals for body weight, simple linear regression).
d – f, Blood metabolic indicators across active and hibernation states. Data represented as mean ± SEM in bar plots. Scatter plots are the same data plotted against days in hibernation and fitted with simple linear regressions.

d, Serum glucose (n = 7 Active and n = 10 IBA animals, Mann-Whitney test, $P < 0.001$).
e, Serum insulin (n = 7 Active and n = 10 IBA animals, student's t-test, $P < 0.0001$).
f, Serum beta-hydroxybutyrate (n = 6 Active and n = 10 IBA animals, student's t-test, $P < 0.0001$).
Each point represents one animal. *$P < 0.05$, **$P < 0.01$, ****$P < 0.0001$.

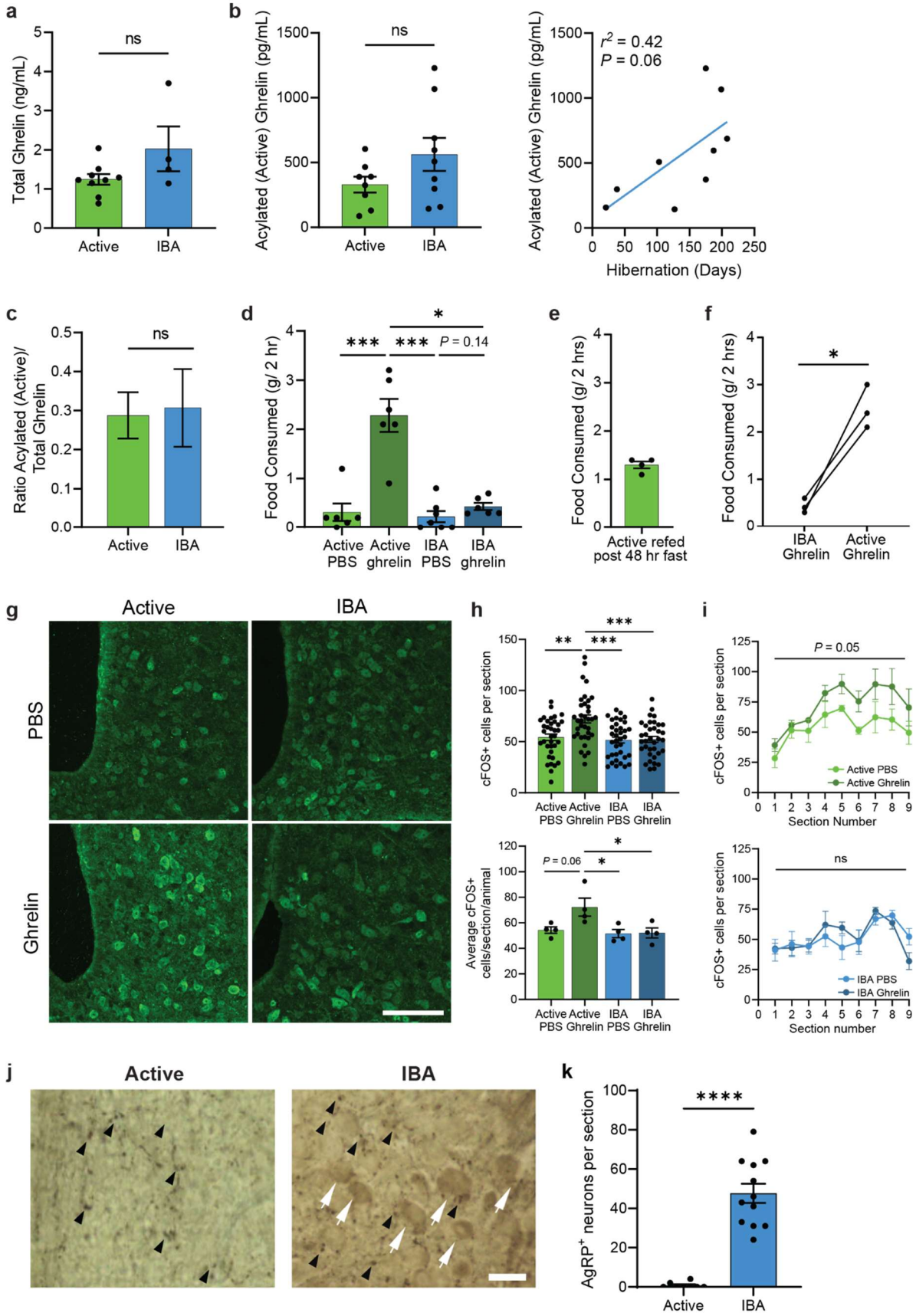

Fig. 2. Hibernating squirrels demonstrate reversible resistance to ghrelin.

a – **c,** Plasma levels of ghrelin across states.
a, Total ghrelin (n = 9 Active and n = 4 IBA animals, mean ± SEM, student's t-test, $P > 0.05$).
b, Acylated (active) ghrelin across states (left, mean ± SEM, student's t-test, $P > 0.05$) and the same data plotted throughout hibernation (right, simple linear regression) (n = 8 Active and n = 9 IBA animals).
c, Ratio of acylated (active):total ghrelin (mean ± SEM, student's t-test, $P > 0.05$, calculated from (**a**) and (**b**)).
d, Two-hour food consumption after ghrelin or PBS injection across states. ($n \geq 6$ animals per group, mean ± SEM, Two-Way ANOVA followed by Tukey's multiple comparisons, State main effect ($F_{1,21} = 5.82$, $P = 0.025$); Treatment main effect ($F_{1,21} = 26.82$, $P < 0.0001$); Interaction ($F_{1,21} = 4.10$, $P = 0.056$).
e, Two-hour food consumption of Active animals following a 48-hour fast. (n = 4 animals, mean ± SEM).
f, Two-hour food consumption of animals during hibernation and following arousal into the active season. (n = 3 animals, student's paired t-test, $P = 0.02$).
g, Representative images of ARC cFOS staining of active and IBA squirrels injected with ghrelin or PBS control. Arrowheads, cFOS+ cells. Scale bar, 100 µm.
h, Quantification of cFOS+ cells per section across ARC volume (top) and average cFOS+ cells per section per animal (bottom) across states after ghrelin injection. (n = 144 sections from 4 animals per group, mean ± SEM, Two-Way ANOVA followed by Tukey's multiple comparisons,(top) State main effect ($F_{1,140} = 5.25$, $P = 0.024$); Treatment main effect ($F_{1,140} = 10.73$, $P = 0.001$); Interaction ($F_{1,140} = 5.23$, $P = 0.024$), (bottom) State main effect ($F_{1,12} = 6.44$, $P = 0.026$); Treatment main effect ($F_{1,12} = 4.24$, $P = 0.062$); Interaction ($F_{1,12} = 3.73$, $P = 0.077$).
i, cFOS+ cells after per section throughout 9 serial sections taken across the volume of the ARC for Active (top) and IBA (bottom) animals after control or ghrelin treatment. Data are the same as (**h**) (top) replotted by section number (mean ± SEM, Two-Way ANOVA followed by Tukey's multiple comparisons, (top) Section number main effect ($F_{2.4,14.4} = 6.67$, $P = 0.007$); Treatment main effect ($F_{1,6} = 5.75$, $P = 0.053$); Interaction ($F_{8,48} = 0.54$, $P = 0.82$), (bottom) Section number main effect ($F_{3.5,20.7} = 4.74$, $P = 0.009$); Treatment main effect ($F_{1,6} = 0.01$, $P = 0.91$); Interaction ($F_{8,48} = 1.12$, $P = 0.37$)).
j, Representative immuno-EM images of ARC from active and IBA animals. White arrows, neuronal soma; black arrowheads, fibers stained for AgRP. Scale bar, 20 µm.
k, Quantification of AgRP+ neuronal soma per section. (n = 8 sections, 3 Active animals and n = 12 sections, 2 IBA animals; mean ± SEM, Mann-Whitney test, $P < 0.0001$).
(**a** – **f, h** bottom) Each point represents one animal. (**h** top**, k**) Each point represents one section. ns = not significiant, $P > 0.05$; $^{**}P < 0.01$; $^{***}P < 0.001$; $^{***}P < 0.0001$.

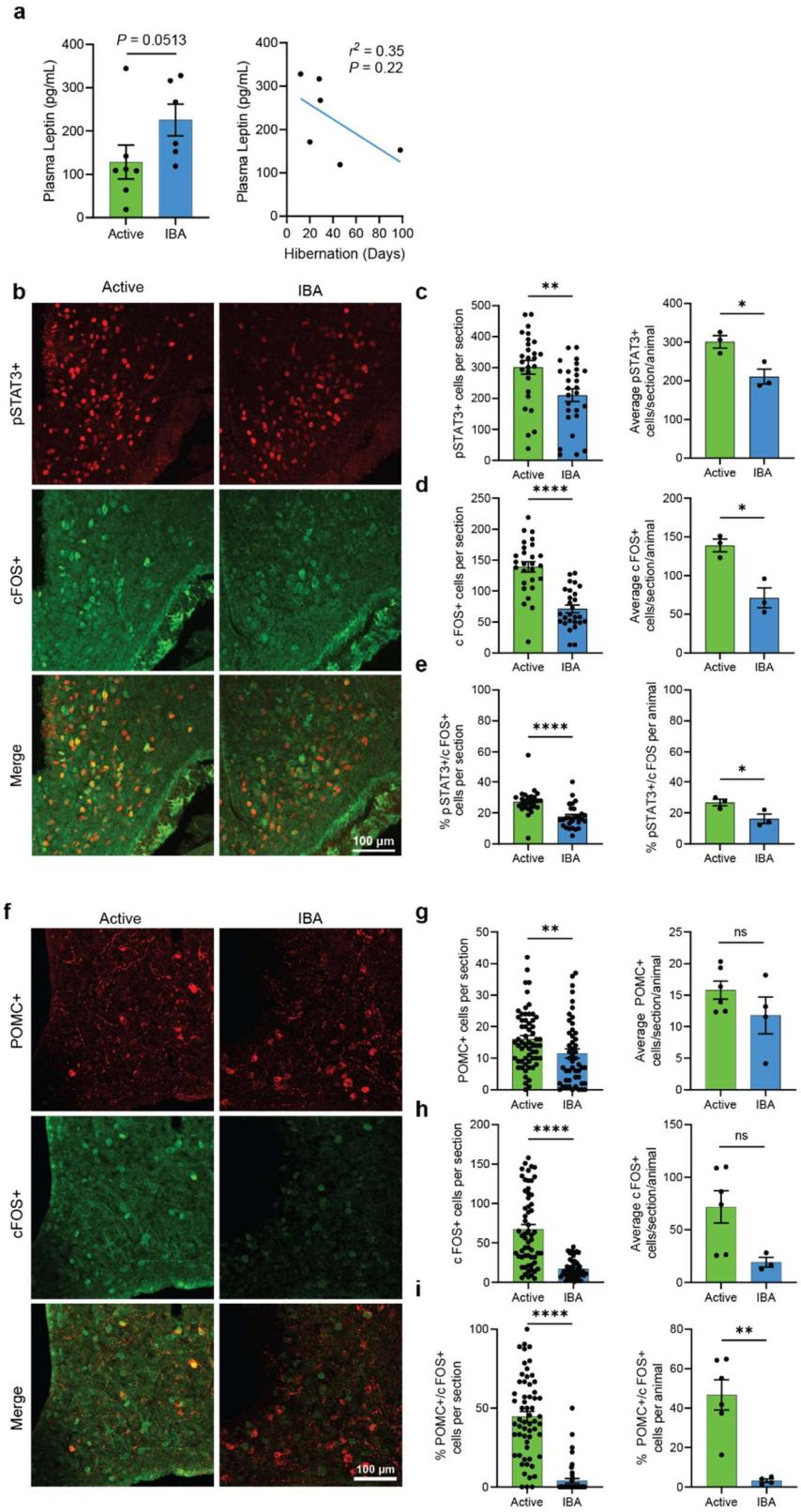

289 **Fig. 3. Hibernating squirrels have reduced leptin signaling.**

a, Plasma leptin levels across states (left, mean ± SEM. Mann-Whitney test, $P = 0.051$) and throughout hibernation (right, simple linear regression) ($n = 7$ active and $n = 6$ IBA animals).
b, Representative immunohistochemistry images of ARC in active and IBA squirrels using anti-pSTAT3 and anti-cFOS antibody. Scale bar, 100 µm.
c – e, Quantification of pSTAT3+ cells (**c**), cFOS+ cells (**d**), and percent pSTAT3+ cells colocalizing cFOS (**e**) by state. (Left) Number of positive cells per section (mean ± SEM; (**c, d**) student's t-test, (**e**) Mann-Whitney test; $P < 0.01$. Each point is one section). (Right) Average number of positive cells per section per animal (mean ± SEM, student's t-test, $P < 0.05$. Each point is one animal). ($n = 27$ sections from 3 active animals and $n = 27$ sections from 3 IBA animals).
f, Representative immunohistochemistry images of ARC in active and IBA squirrels using anti-POMC and anti-cFOS antibody. Scale bar, 100 µm.
g – i, Quantification of POMC+ cells (**g**), cFOS+ cells (**h**), and percent POMC+ cells colocalizing with cFOS (**i**) by state. (Left) Number of positive cells per section (mean ± SEM, Mann-Whitney test, $P < 0.01$. Each point is one section). (Right) Average number of positive cells per section per animal (mean ± SEM, student's t-test, (**g, h**) $P > 0.05$, (**i**) $P < 0.01$. Each point is one animal). ($n = 60$ sections from 6 active animals and $n = 50$ sections from 4 IBA animals)
n.s. = not significant, $P > 0.05$; *$P < 0.05$; **$P < 0.01$; ****$P < 0.0001$.

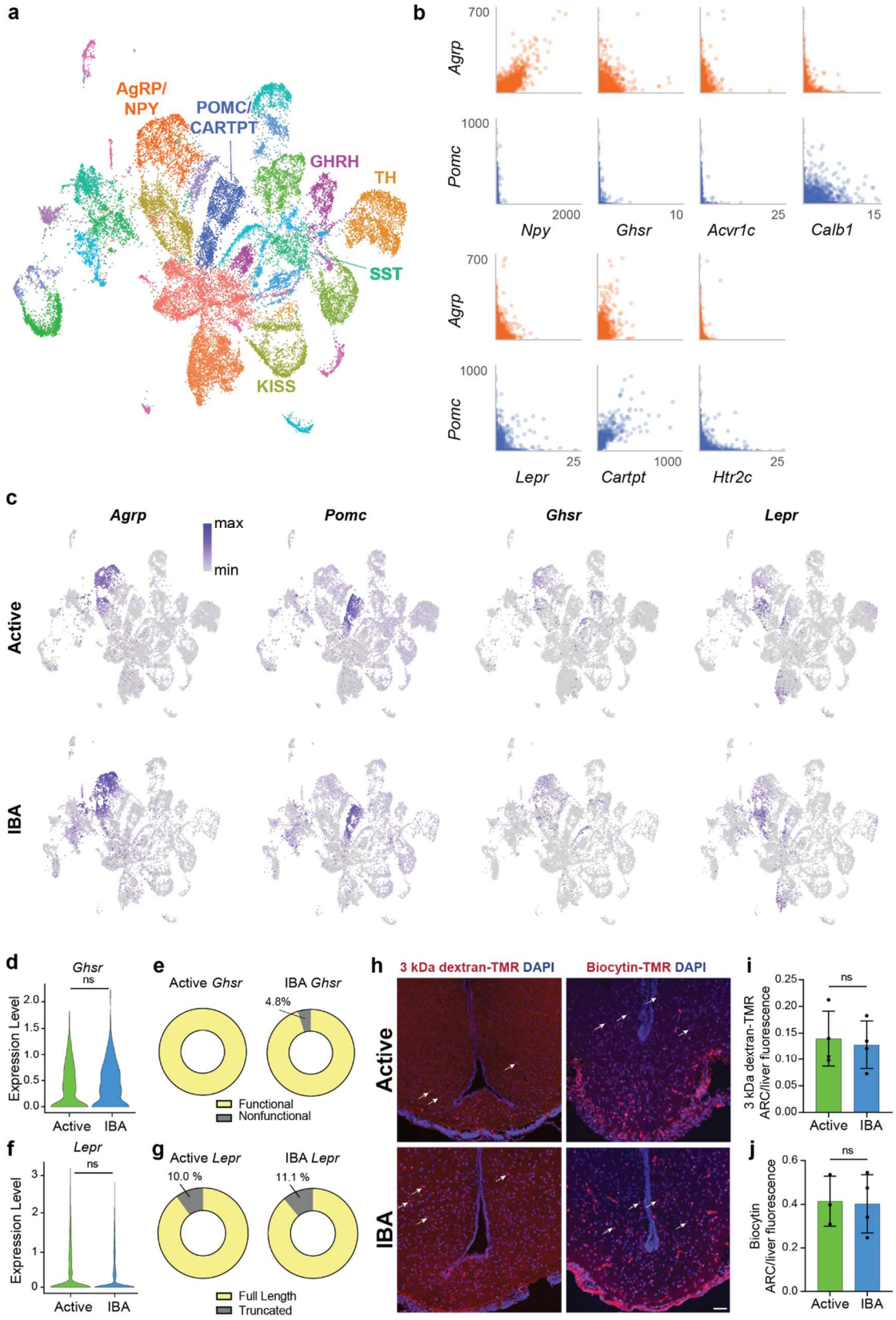

Fig. 4. Ghrelin and leptin receptors expression and blood brain barrier function are unaltered during hibernation.

a, 2-dimensional UMAP projection of gene expression in individual arcuate nucleus and median eminence (ARC-ME) neurons colored by cluster (*n* = integration from 3 active and *n* = integration from 3 IBA animals).
b, Coexpression of *Agrp* and *Pomc* with known markers of AgRP and POMC neurons. Values are in counts per 10,000 total counts.
c, Expression of *Agrp, Pomc, Ghsr, and Lepr genes* in individual ARC-ME neurons in Active and IBA states (normalized, log-transformed, and represented by color as indicated in the color bar).
d, Expression of *Ghsr* in AgRP neurons across states (Wilcoxon rank sum test (R/Seurat), $P > 0.05$).
e, Quantification of functional versus nonfunctional *Ghsr* isoforms from de novo cloning across states ($n \geq 38$ clones from 2 animals per state).
f, Expression of *Lepr* in POMC neurons across states (Wilcoxon rank sum test (R/Seurat), $P > 0.05$).
g, Quantification of truncated versus full length long-form leptin-receptor from de novo cloning across states ($n \geq 9$ clones from 2 animals per state).
h – **j,** Blood brain permeability assays by tail artery injection in active and IBA squirrels of 3kDa dextran-tetramethylrhodamine (TMR) and 860 Da biocytin-TMR.
h, Representative images of ARC-ME demonstrating deposition of dye (white arrows). Scale bar, 50 µm.
i – **j**, Quantification of normalized fluorescence of 3kDa dextran-TMR (**i**, *n* = 4 active and *n* = 4 IBA animals, mean ± SEM, student's t-test, $P > 0.05$) and 860 Da biocytin-TMR (**j**, *n* = 3 active and *n* = 4 IBA animals, mean ± SEM, student's t-test, $P > 0.05$).
Each point represents one animal. ns = not significant, $P < 0.05$.

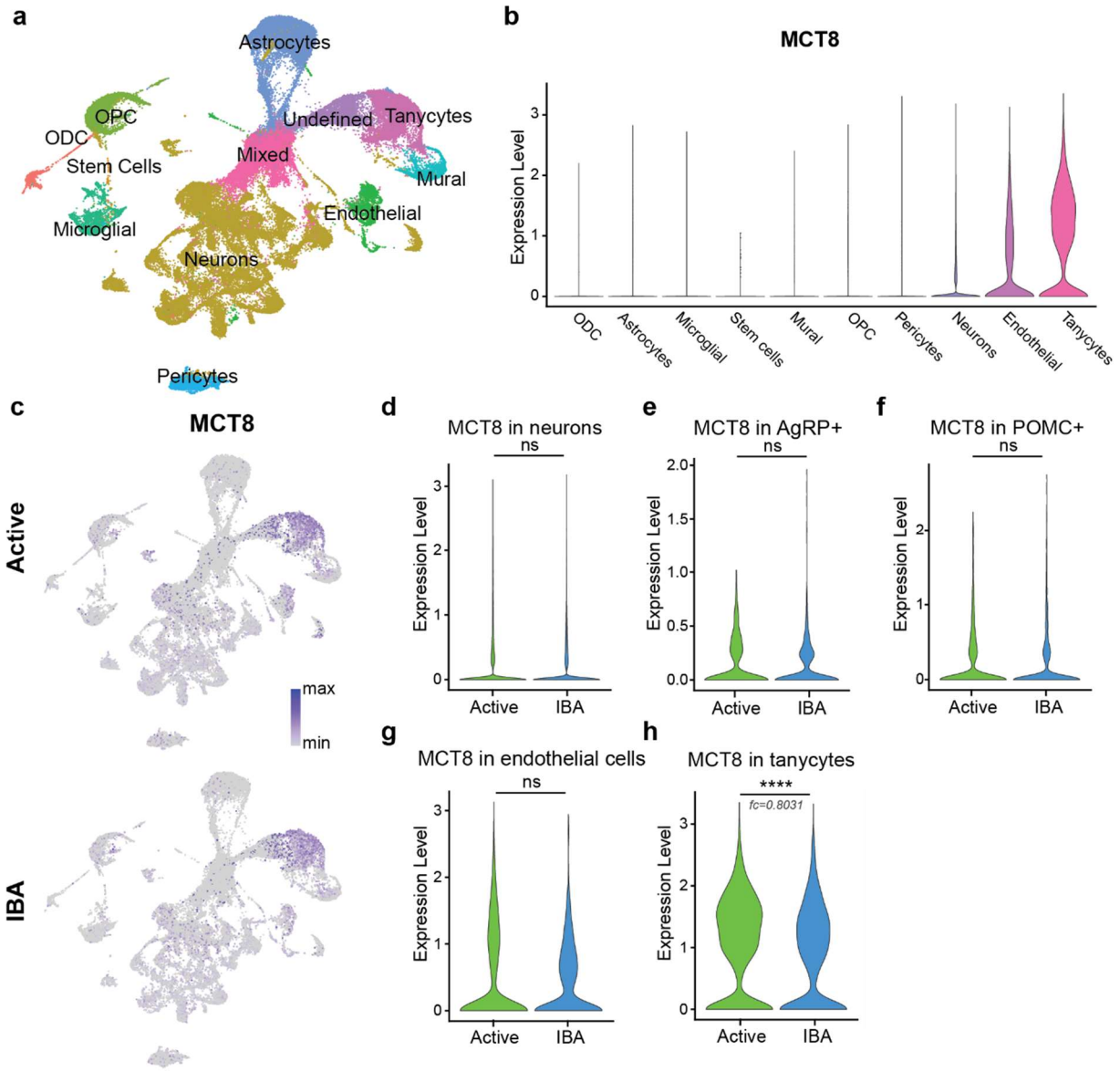

Fig. 5. Thyroid hormone transporter MCT8 is downregulated in tanycytes during hibernation
a, 2-dimensional UMAP projection of gene expression in individual arcuate nucleus and median eminence (ARC-ME) cells, colored by cell type, as determined by clustering and annotation.
b – **c,** Expression of *MCT8* in identified cell types, aggregated for both states (**b**, violin plots) and separated by state (**c**, UMAP plots).
d – **h,** Expression of *MCT8* across states in all neurons (**d**), AgRP neurons (**e**), POMC neurons (**f**), endothelial cells (**g**), and tanycytes (**h**). Violin plots show normalized log-transformed gene counts. (Wilcoxon rank sum test (R/Seurat), (**d** - **g**) $P > 0.05$, (**h**) $P < 0.0001$.)
ns = not significant, $P > 0.05$; ****$P < 0.0001$; fc = fold count.

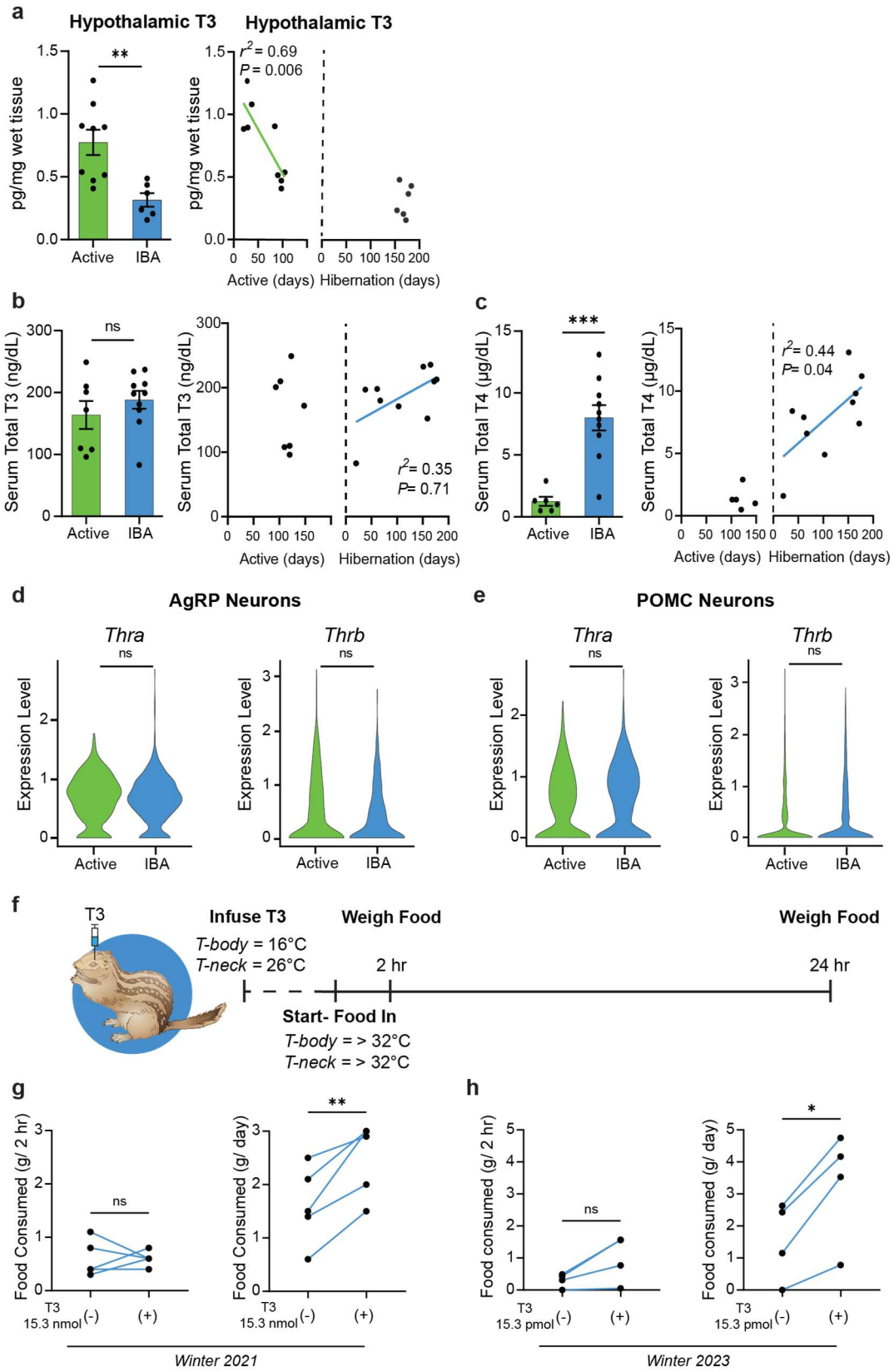

339 **Fig. 6. Reversible central hypothyroidism underlies hibernation anorexia.**

340 **a,** T3 content measured from homogenized hypothalamus from active and IBA squirrels (left,
341 mean ± SEM, student's t-test, $P < 0.01$), and plotted by days active and days in hibernation (right,
342 simple linear regression) ($n = 9$ Active and $n = 6$ IBA animals).
343 **b** – **c,** Serum total thyroid hormone concentration across active and IBA seasons (left, mean ±
344 SEM) and plotted by days active and days in hibernation (right, simple linear regression).
345 **b,** Total T3 ($n = 7$ Active and $n = 10$ IBA animals, student's t-test, $P > 0.05$).
346 **c,** Total T4 ($n = 6$ Active and $n = 10$ IBA animals, student's t-test, $P < 0.001$).
347 **d** – **e,** Expression of *Thra* and *Thrb* in AgRP neurons (**d**) and POMC neurons (**e**) by single cell RNA
348 sequencing. Violin plots show normalized log-transformed gene counts. Wilcoxon rank sum test
349 (R/Seurat, $P > 0.05$).
350 **f** – **i,** Hypothalamic infusion of T3 during IBA and resulting food consumption.
351 **f,** Schematic of hypothalamic T3 infusion during IBA after arousal from torpor.
352 **g** – **h,** Paired food consumption at two-hours (left) and 24-hours (right) after control and
353 hypothalamic infusion of (**g**), 15.3 nmol T3 ($n = 5$ animals, paired student's t-test, (left) $P > 0.05$,
354 (right) $P < 0.01$ and (**h**), 15.3 pmol T3 ($n = 4$ animals, paired student's t-test, (left) $P > 0.05$, (right)
355 $P < 0.05$).
356 Each point represents one animal. ns = not significant, $P > 0.05$; $^{**}P < 0.01$; $^{****}P < 0.0001$.

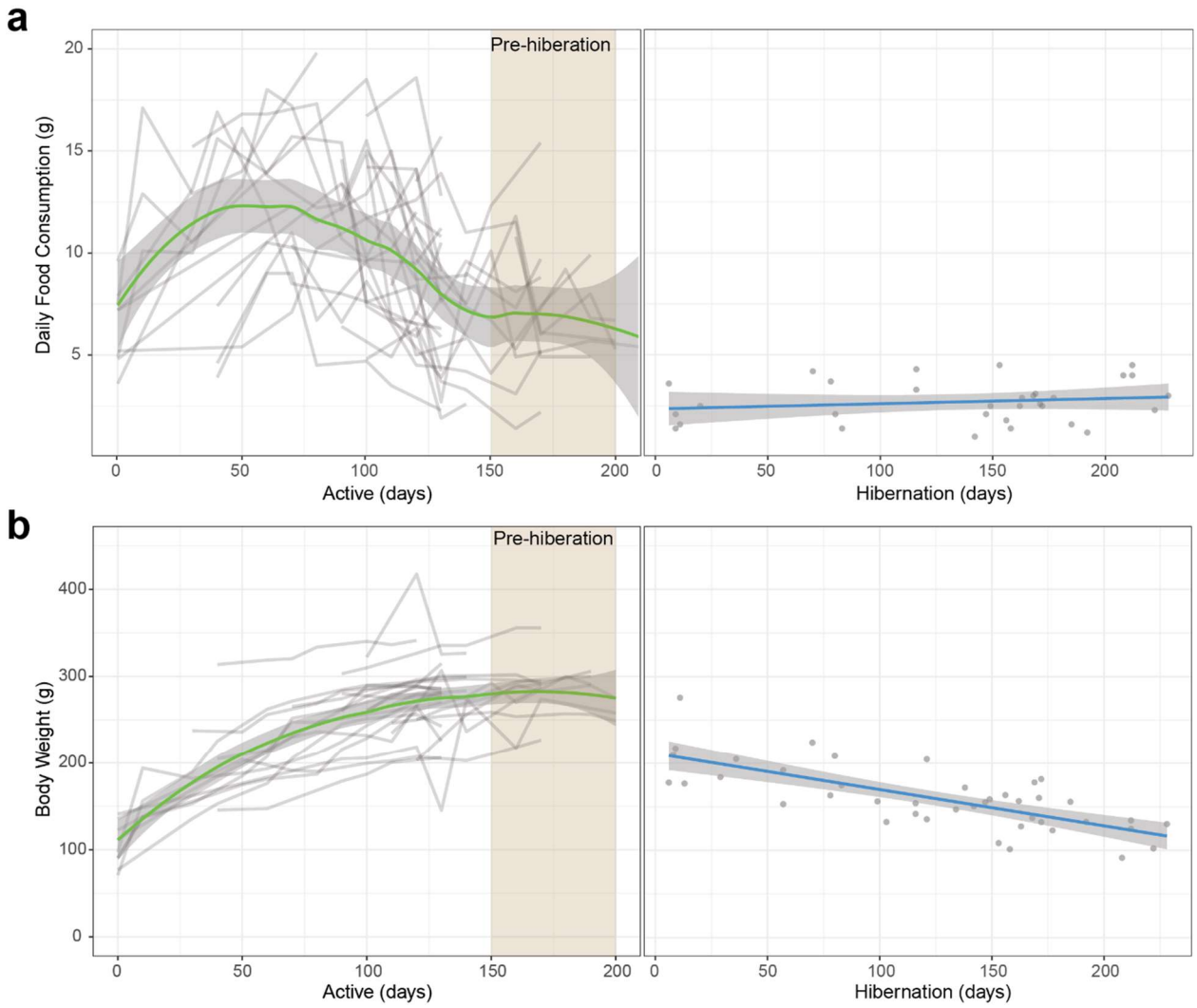

Extended Data Fig. 1. Seasonal feeding and body weight changes.
Daily food consumption (**a**) and body weight (**b**) of squirrels plotted by days active and days in hibernation. Food consumption and body weight was assessed serially within animals across active season into pre-hibernation, with each line representing one squirrel (*n* = 25 active and *n* = 25 pre-hibernation animals). IBA feeding and body weight was assessed only once per hibernation season per squirrel, with each point representing one squirrel (*n* = 36 IBA animals for food measurement and *n* = 42 animals for body weight measurement). Active data was fit with a loess regression and hibernating data was fit with a simple linear regression.

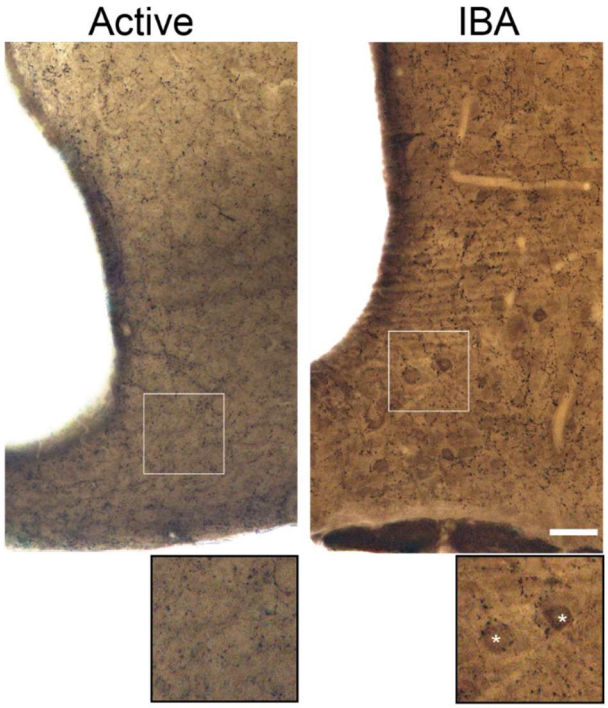

Extended Data Fig. 2. Immunoelectron microscopy of AgRP neurons.
Representative immunoelectron microscopy images demonstrating AgRP+ staining in the neuronal somas of IBA ARC neurons only. Asterisks indicate neuronal soma. Scale bar = 50 µm.

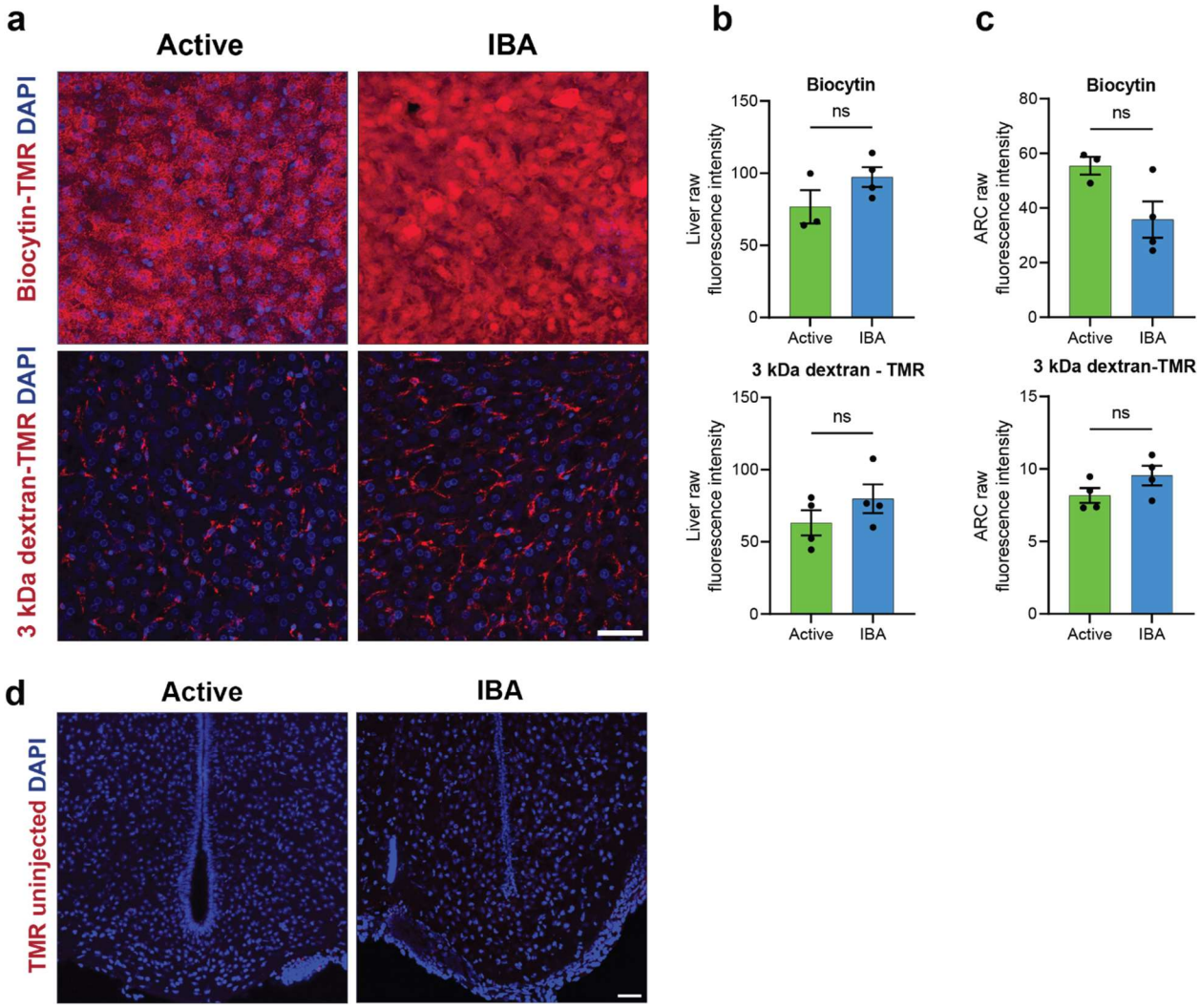

Extended Data Fig. 3. Raw fluorescence and uninjected controls for blood brain barrier permeability assays.

a, Representative immunohistochemistry images of liver across states after tail artery injection of 860 Da biocytin-TMR and 3kDa dextran-tetramethylrhodamine (TMR). Scale bar, 50 µm.

b - **c**, Raw fluorescence intensity of dye in liver (**b**) and arcuate nucleus and median eminence (**c**) across states (mean ± SEM, each point represents one animal, dextran: n = 4 and n = 4 IBA animals; biocytin: n = 3 active and n = 4 IBA animals, student's t-test, $P > 0.05$). Note that representative immunohistochemistry images of the ARC-ME after dye injection are shown in Main Fig 4h.

d, Representative images demonstrating lack of fluorescence in animals that were not injected with dye. Scale bar, 50 µm.

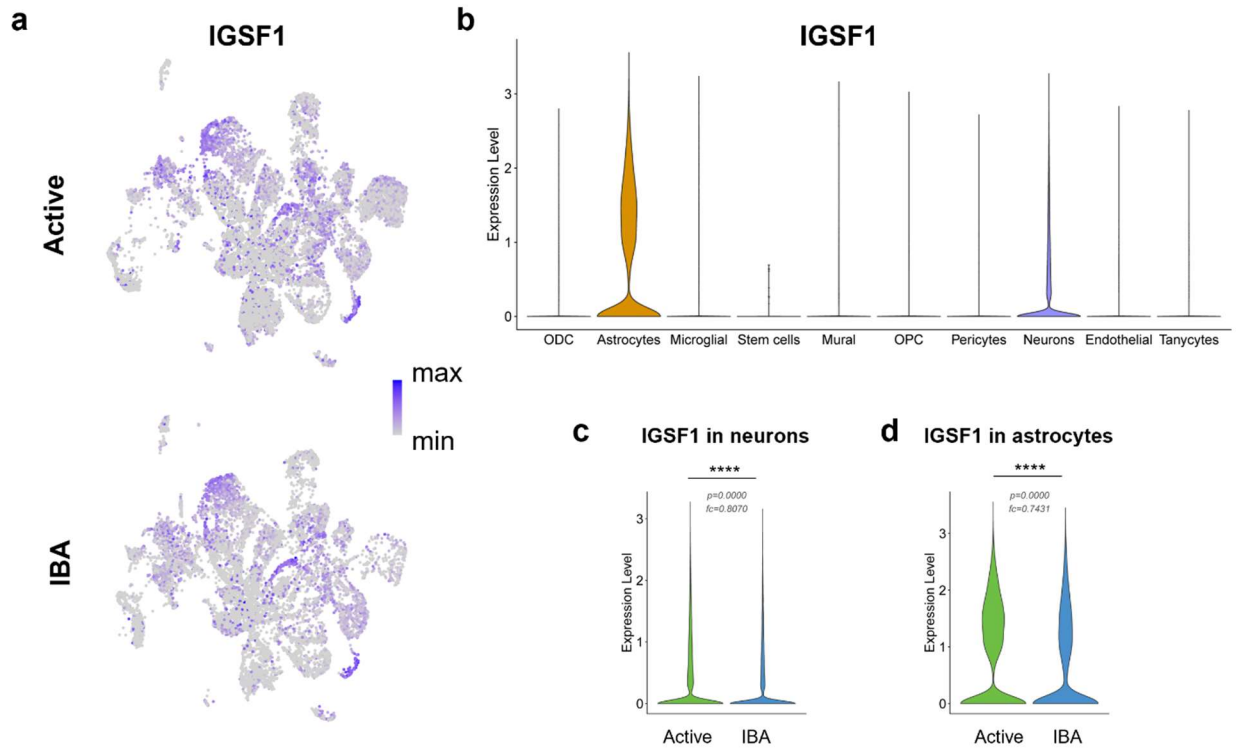

Extended Data Fig. 4. IGSF1 is downregulated in ARC neurons during hibernation

a, 2-dimensional UMAP projection of *Igsf1* gene expression in individual arcuate nucleus and median eminence (ARC-ME) cells (normalized, log-transformed, and represented by color as indicated in the color bar).

b, Violin plots showing Expression of *IGSF1* in identified cell types aggregated for both states.

c, d, Expression of *Igsf1* across states in all neurons (**c**) and astrocytes (**d**). Violin plots show normalized log-transformed gene counts. (Wilcoxon rank sum test (R/Seurat). ****$P < 0.0001$).

Cluster	NumCells	PercentCells	Marker1	Marker2	Marker3
0	3766	11.93	NRXN3	LRRTM4	DCC
1	2916	9.24	TENM2	LDB2	CLSTN2
2	2246	7.11	TAC1	ADCYAP1	PENK
3	1912	6.06	POMC	CARTPT	SHISAL2B
4	1744	5.52	NPY	AGRP	CARTPT
5	1678	5.32	GRIK1	SGCZ	NEK10
6	1450	4.59	KISS1	TAC3	ESR1
7	1429	4.53	GAD2	TCF7L2	ALCAM
8	1419	4.49	TRHDE	RELN	GAL
9	1377	4.36	C8orf34	SATB2	TH
10	1334	4.23	TRPM3	PDE7B	LAMA3
11	1237	3.92	ENSSTOG00000024849	SLC1A3	CST3[mh]
12	998	3.16	TRH	SST	NTS
13	992	3.14	SLC4A4	SLC6A11	SPARCL1
14	895	2.84	PDE3A	SPHKAP	PPP1R17
15	731	2.32	GHRH	GAL	NKAIN3
16	710	2.25	APOD	PTGDS	DCN
17	662	2.1	NTS	CACNA2D3	NXPH1
18	560	1.77	PMCH	HCRT	GAL
19	548	1.74	PPP1R17	CCK	PDYN
20	547	1.73	CGA	CHGA	KRT27
21	521	1.65	CSRP2	OTP	HTATSF1
22	455	1.44	PDGFRA	FABP7	TF
23	367	1.16	MKX	NCALD	TMSB4X
24	342	1.08	TAC3	GAL	IGSF1
25	292	0.92	IGFBP5	RBPMS	MGP
26	254	0.8	TAC1	FOXP2	EPHA6
27	123	0.39	AVP	OXT.1[mh]	OXT[mh]
28	64	0.2	C1QA	C1QC	TYROBP

Extended Data Table 1. Top markers of neuronal clusters.
Top three markers of the 29 identified neuronal clusters.

References

1. Hays, N. P. & Roberts, S. B. The anorexia of aging in humans. *Physiol. Behav.* **88**, 257–266 (2006).
2. Talbert, E. E. & Guttridge, D. C. Emerging Signaling Mediators in the Anorexia-Cachexia Syndrome of Cancer. *Trends Cancer* **8**, 397–403 (2022).
3. Bulik, C. M., Carroll, I. M. & Mehler, P. Reframing Anorexia Nervosa as a Metabo-Psychiatric Disorder. *Trends Endocrinol. Metab. TEM* **32**, 752–761 (2021).
4. Watson, H. J. *et al.* Genome-wide Association Study Identifies Eight Risk Loci and Implicates Metabo-Psychiatric Origins for Anorexia Nervosa. *Nat. Genet.* **51**, 1207–1214 (2019).
5. Fortin, S. M. *et al.* GABA neurons in the nucleus tractus solitarius express GLP-1 receptors and mediate anorectic effects of liraglutide in rats. *Sci. Transl. Med.* **12**, eaay8071 (2020).
6. Sweeney, P. *et al.* The melanocortin-3 receptor is a pharmacological target for the regulation of anorexia. *Sci. Transl. Med.* **13**, eabd6434 (2021).
7. Andrews, M. T. Molecular interactions underpinning the phenotype of hibernation in mammals. *J. Exp. Biol.* **222**, jeb160606 (2019).
8. Healy, J. E., Bateman, J. L., Ostrom, C. E. & Florant, G. L. Peripheral ghrelin stimulates feeding behavior and positive energy balance in a sciurid hibernator. *Horm. Behav.* **59**, 512–519 (2011).
9. Mrosovsky, N. & Boshes, M. Meal patterns and food intakes of ground squirrels during circannual cycles. *Appetite* **7**, 163–175 (1986).
10. Torke, K. G. & Twente, J. W. Behavior of Spermophilus lateralis between Periods of Hibernation. *J. Mammal.* **58**, 385–390 (1977).
11. Pulawa, L. K. & Florant, G. L. The Effects of Caloric Restriction on the Body Composition and Hibernation of the Golden-Mantled Ground Squirrel (Spermophilus lateralis). *Physiol. Biochem. Zool.* **73**, 538–546 (2000).
12. Cowley, M. A. *et al.* The Distribution and Mechanism of Action of Ghrelin in the CNS Demonstrates a Novel Hypothalamic Circuit Regulating Energy Homeostasis. *Neuron* **37**, 649–661 (2003).
13. Gropp, E. *et al.* Agouti-related peptide–expressing neurons are mandatory for feeding. *Nat. Neurosci.* **8**, 1289–1291 (2005).
14. Hahn, T. M., Breininger, J. F., Baskin, D. G. & Schwartz, M. W. Coexpression of Agrp and NPY in fasting-activated hypothalamic neurons. *Nat. Neurosci.* **1**, 271–272 (1998).
15. Kojima, M. *et al.* Ghrelin is a growth-hormone-releasing acylated peptide from stomach. *Nature* **402**, 656–660 (1999).
16. Toshinai, K. *et al.* Upregulation of Ghrelin Expression in the Stomach upon Fasting, Insulin-Induced Hypoglycemia, and Leptin Administration. *Biochem. Biophys. Res. Commun.* **281**, 1220–1225 (2001).
17. Bradley, S. P., Pattullo, L. M., Patel, P. N. & Prendergast, B. J. Photoperiodic regulation of the orexigenic effects of ghrelin in Siberian hamsters. *Horm. Behav.* **58**, 647–652 (2010).
18. Nakazato, M. *et al.* A role for ghrelin in the central regulation of feeding. *Nature* **409**, 194–198 (2001).
19. Wren, A. M. *et al.* The Novel Hypothalamic Peptide Ghrelin Stimulates Food Intake and Growth Hormone Secretion. *Endocrinology* **141**, 4325–4328 (2000).
20. Asakawa, A. *et al.* Ghrelin is an appetite-stimulatory signal from stomach with structural resemblance to motilin. *Gastroenterology* **120**, 337–345 (2001).
21. Sun, Y., Wang, P., Zheng, H. & Smith, R. G. Ghrelin stimulation of growth hormone release and appetite is mediated through the growth hormone secretagogue receptor. *Proc. Natl. Acad. Sci.* **101**, 4679–4684 (2004).
22. Nogueiras, R. *et al.* Bsx, a Novel Hypothalamic Factor Linking Feeding with Locomotor Activity, Is Regulated by Energy Availability. *Endocrinology* **149**, 3009–3015 (2008).
23. Chen, H. Y. *et al.* Orexigenic Action of Peripheral Ghrelin Is Mediated by Neuropeptide Y and Agouti-Related Protein. *Endocrinology* **145**, 2607–2612 (2004).

24. Yanagi, S., Sato, T., Kangawa, K. & Nakazato, M. The Homeostatic Force of Ghrelin. *Cell Metab.* **27**, 786–804 (2018).
25. Sakkou, M. *et al.* A Role for Brain-Specific Homeobox Factor Bsx in the Control of Hyperphagia and Locomotory Behavior. *Cell Metab.* **5**, 450–463 (2007).
26. Vaisse, C. *et al.* Leptin activation of Stat3 in the hypothalamus of wild–type and ob/ob mice but not db/db mice. *Nat. Genet.* **14**, 95–97 (1996).
27. Zhan, C. *et al.* Acute and Long-Term Suppression of Feeding Behavior by POMC Neurons in the Brainstem and Hypothalamus, Respectively. *J. Neurosci.* **33**, 3624–3632 (2013).
28. Krashes, M. J., Lowell, B. B. & Garfield, A. S. Melanocortin-4 receptor–regulated energy homeostasis. *Nat. Neurosci.* **19**, 206–219 (2016).
29. Campbell, J. N. *et al.* A Molecular Census of Arcuate Hypothalamus and Median Eminence Cell Types. *Nat. Neurosci.* **20**, 484–496 (2017).
30. Gorska, E. *et al.* Leptin receptors. *Eur. J. Med. Res.* **15**, 50–54 (2010).
31. Kong, W. M. *et al.* Triiodothyronine Stimulates Food Intake via the Hypothalamic Ventromedial Nucleus Independent of Changes in Energy Expenditure. *Endocrinology* **145**, 5252–5258 (2004).
32. Varela, L. *et al.* Hypothalamic mTOR pathway mediates thyroid hormone-induced hyperphagia in hyperthyroidism. *J. Pathol.* **227**, 209–222 (2012).
33. Amin, A., Dhillo, W. S. & Murphy, K. G. The Central Effects of Thyroid Hormones on Appetite. *J. Thyroid Res.* **2011**, (2011).
34. Diano, S., Naftolin, F., Goglia, F. & Horvath, T. L. Fasting-Induced Increase in Type II Iodothyronine Deiodinase Activity and Messenger Ribonucleic Acid Levels Is Not Reversed by Thyroxine in the Rat Hypothalamus*. *Endocrinology* **139**, 2879–2884 (1998).
35. Diano, S., Naftolin, F., Goglia, F., Csernus, V. & Horvath, T. L. Monosynaptic Pathway Between the Arcuate Nucleus Expressing Glial Type II Iodothyronine 5′-Deiodinase mRNA and the Median Eminence-Projective TRH Cells of the Rat Paraventricular Nucleus. *J. Neuroendocrinol.* **10**, 731–742 (1998).
36. Coppola, A. *et al.* A Central Thermogenic-like Mechanism in Feeding Regulation: An Interplay between Arcuate Nucleus T3 and UCP2. *Cell Metab.* **5**, 21–33 (2007).
37. Andrews, Z. B. *et al.* UCP2 mediates ghrelin's action on NPY/AgRP neurons by lowering free radicals. *Nature* **454**, 846–851 (2008).
38. Wirth, E. K. *et al.* Neuronal 3′,3,5-Triiodothyronine (T3) Uptake and Behavioral Phenotype of Mice Deficient in Mct8, the Neuronal T3 Transporter Mutated in Allan–Herndon–Dudley Syndrome. *J. Neurosci.* **29**, 9439–9449 (2009).
39. Roberts, L. M. *et al.* Expression of the Thyroid Hormone Transporters Monocarboxylate Transporter-8 (SLC16A2) and Organic Ion Transporter-14 (SLCO1C1) at the Blood-Brain Barrier. *Endocrinology* **149**, 6251–6261 (2008).
40. Braun, D. *et al.* Developmental and cell type-specific expression of thyroid hormone transporters in the mouse brain and in primary brain cells. *Glia* **59**, 463–471 (2011).
41. Sun, Y. *et al.* Loss-of-function mutations in IGSF1 cause an X-linked syndrome of central hypothyroidism and testicular enlargement. *Nat. Genet.* **44**, 1375–1381 (2012).
42. Brûlé, E. *et al.* IGSF1 Deficiency Leads to Reduced TSH Production Independent of Alterations in Thyroid Hormone Action in Male Mice. *Endocrinology* **163**, bqac092 (2022).
43. García, M. *et al.* The syndrome of central hypothyroidism and macroorchidism: IGSF1 controls TRHR and FSHB expression by differential modulation of pituitary TGFβ and Activin pathways. *Sci. Rep.* **7**, 42937 (2017).
44. Joustra, S. D. *et al.* The IGSF1 Deficiency Syndrome: Characteristics of Male and Female Patients. *J. Clin. Endocrinol. Metab.* **98**, 4942–4952 (2013).

45. Boelen, A., van Trotsenburg, A. S. P. & Fliers, E. Chapter 10 - Congenital isolated central hypothyroidism: Novel mutations and their functional implications. in *Handbook of Clinical Neurology* (eds. Swaab, D. F., Kreier, F., Lucassen, P. J., Salehi, A. & Buijs, R. M.) vol. 180 161–169 (Elsevier, 2021).
46. Mullur, R., Liu, Y.-Y. & Brent, G. A. Thyroid Hormone Regulation of Metabolism. *Physiol. Rev.* **94**, 355–382 (2014).
47. Aristotle. *The History of Animals*. vol. Book 8, Part 13-17 (The Internet Classics Archive, 350AD).
48. Mohr, S. M., Bagriantsev, S. N. & Gracheva, E. O. Cellular, Molecular, and Physiological Adaptations of Hibernation: The Solution to Environmental Challenges. *Annu. Rev. Cell Dev. Biol.* **36**, 315–338 (2020).
49. Ettleson, M. D. & Papaleontiou, M. Evaluating health outcomes in the treatment of hypothyroidism. *Front. Endocrinol.* **13**, 1026262 (2022).
50. Fenneman, A. C., Bruinstroop, E., Nieuwdorp, M., van der Spek, A. H. & Boelen, A. A comprehensive review of thyroid hormone metabolism in the gut and its clinical implications. *Thyroid* (2022) doi:10.1089/thy.2022.0491.
51. Barrett, P. *et al.* Hypothalamic Thyroid Hormone Catabolism Acts as a Gatekeeper for the Seasonal Control of Body Weight and Reproduction. *Endocrinology* **148**, 3608–3617 (2007).
52. Herwig, A. *et al.* Photoperiod and acute energy deficits interact on components of the thyroid hormone system in hypothalamic tanycytes of the Siberian hamster. *Am. J. Physiol.-Regul. Integr. Comp. Physiol.* **296**, R1307–R1315 (2009).
53. Murphy, M. *et al.* Effects of Manipulating Hypothalamic Triiodothyronine Concentrations on Seasonal Body Weight and Torpor Cycles in Siberian Hamsters. *Endocrinology* **153**, 101–112 (2012).
54. Dardente, H., Hazlerigg, D. G. & Ebling, F. J. P. Thyroid hormone and seasonal rhythmicity. *Front. Endocrinol.* **5**, 19 (2014).
55. Chmura, H. E. *et al.* Hypothalamic remodeling of thyroid hormone signaling during hibernation in the arctic ground squirrel. *Commun. Biol.* **5**, 1–13 (2022).
56. Grijota-Martínez, C., Bárez-López, S., Gómez-Andrés, D. & Guadaño-Ferraz, A. MCT8 Deficiency: The Road to Therapies for a Rare Disease. *Front. Neurosci.* **14**, 380 (2020).
57. Friesema, E. C. *et al.* Association between mutations in a thyroid hormone transporter and severe X-linked psychomotor retardation. *The Lancet* **364**, 1435–1437 (2004).
58. Mayerl, S. *et al.* Transporters MCT8 and OATP1C1 maintain murine brain thyroid hormone homeostasis. *J. Clin. Invest.* **124**, 1987–1999 (2014).

Methods

Animals

All experimental procedures were performed in compliance with the Institutional Animal Care and Use Committee of Yale University (protocol 2021-11497). Thirteen-lined ground squirrels (*Ictidomys tridecemlineatus*) were obtained from Dr. Dana Merriman (University of Wisconsin-Oshkosh) and/or bred in our facilities (Yale University). Animals (age 0.5 – 3 years) of both sexes were single housed in temperature- and humidity-controlled facilities at Yale University. All squirrels were implanted with an interscapular temperature transponder (IPTT-300, BMDS).

During the active season (May – August), squirrels were kept in a vivarium at 21 ± 1 °C under a 12 hour:12 hour light:dark cycle at 40 – 60% humidity and maintained on a diet of dog food (IAMS) supplemented with sunflower seeds, superworms, and fresh vegetables (celery and carrots) with *ad libitum* access to water.

During the fall pre-hibernation season (September – October), squirrels were kept in a vivarium at 20 ± 1 °C under a light:dark cycle matched to Central Standard Time sunrise:sunset, which corresponds to the native time zone of thirteen-lined ground squirrels. Animals were kept at 40 – 60% humidity and maintained on a diet of dog food (IAMS) supplemented with sunflower seeds with *ad libitum* access to water.

During hibernation season (September – April), hypothermic squirrels (body temperature ~20 ± 1 °C) were moved to the hibernaculum, which was kept at 4°C at 40 – 60% humidity under constant darkness, without access to food or water.

In this study, "active" squirrels were those with a constant core body temperature (CBT) of 37 °C during the active season. "Pre-hibernation" squirrels were those that generally maintained euthermic, but also demonstrated transient, hypothermic bouts to ~20 °C. "IBA" squirrels were those who had undergone at least one bout of hypothermic torpor during the hibernation season but had achieved a CBT of > 32 °C for ≥ 60 minutes, or ≥ 20 minutes for the central thyroid hormone experiments.

Food Consumption and Body Mass Measurement

Food consumption and body weight of adult animals were measured every 2 weeks during the active period (May-August) and into the pre-hibernation season (September – October). Active and pre-hibernation animals were moved to the behavioral room kept at 20 ± 1°C under a 12 hour:12 hour light:dark cycle and acclimated overnight. In the morning (9 – 11 AM), each was weighed, transferred to a clean cage, and allowed to habituate for 30 minutes. Food consumption measurements were performed with dog food only. Pre-weighed food was added to each cage, and animals were allowed to feed undisturbed. Food remaining 24 hours later was weighed and used to calculate daily food consumption. A separate bowl of dog food was kept in the behavior room to control for weight changes due to ambient humidity, but no difference was found so no correction was needed. The maximum food consumption per animal for the active season was reported. Pre-hibernation feeding data corresponds to the last 24-hr period in the pre-hibernation season where animals maintain euthermia for the duration of the experiment.

555 Hibernating animals entered IBA spontaneously, so their food consumption and body
556 weight measurements occurred between 11 AM – 8 PM. IBA animals were weighed, transferred
557 to a clean cage in the hibernaculum kept at 4°C under constant darkness and allowed to habituate
558 for 30 minutes. Food consumption measurements were performed with dog food only. Pre-
559 weighed food was added to each cage, and animals were allowed to feed undisturbed. Food
560 remaining 24 hours later was weighed and used to calculate daily food consumption. IBA
561 measurements occurred just once during the hibernation season, to ensure that animals
562 remained naïve to food availability during the winter. A separate bowl of dog food was kept in
563 the behavior room, kept at 4°C in constant darkness, to control for weight changes due to
564 ambient humidity, but no difference was found so no correction was needed.

565 **Blood collection**

566 Animals were euthanized by isoflurane overdose. The chest cavity was opened, the right
567 atrium of the heart pierced, and trunk blood was collected with a 18G needle and syringe.

568 **Serum hormone and metabolite measurements**

569 Whole blood was allowed to coagulate at room temperature for 30 minutes, then
570 centrifuged at 4°C at 2000 rcf for 15 minutes. Serum was aliquoted and stored at -80°C for later
571 use. Serum glucose, insulin, beta-hydroxybutyrate, total T3, and total T4 measurement were
572 performed by Antech Diagnostics (Fountain Valley, CA).

573 **Plasma ghrelin measurements**

574 Whole blood was collected into chilled, pre-coated K_3 EDTA tubes (MiniCollect, Grenier
575 Bio-One) and immediately treated with Pefabloc (Sigma) to a final concentration of 1 mM. Blood
576 was centrifuged at 1600 rcf for 15 minutes. Plasma was aliquoted and stored at -80°C for later
577 use. Plasma active (acylated) ghrelin was measured by mouse/rat ELISA (EZRGRA-90K, Millipore).
578 Plasma total ghrelin was measured by mouse/rat ELISA (EZRGRT-91K, Millipore). All samples were
579 run in duplicate. The ratio of acylated (active form of ghrelin)/ total ghrelin was calculated by
580 dividing the mean of the acylated ghrelin concentration by the mean of the total ghrelin
581 concentration per state. The SEM of the ratio was calculated by simple error propagation given
582 by the formula:

583 $\sigma_{ratio} = sqrt\ ((\sigma A/A)2\ +\ (\sigma B/B)2\ ))\ *\ A/B$

584 where A and B are mean values of active (acylated) and total ghrelin, respectively.

585 **Plasma leptin measurements**

586 Whole blood was collected into chilled, pre-coated K_2EDTA tubes (BD Vacutainer,
587 Lavender/H) and immediately treated with aprotinin (Millipore Sigma, 9087-70-1) to a final
588 concentration of 0.02 mM. Blood was centrifuged at 1600 rcf for 15 minutes. Plasma was
589 aliquoted and stored at -80°C for later use. Plasma leptin was measured by mouse/rat ELISA (R&D
590 Systems, MOB00). All samples were run in duplicate. A ROUT outlier test (Q = 1 %) was run to
591 identify one outlier in the Active state and two outliers in the IBA state.

592 **Intraperitoneal Ghrelin injections**

593 Ground squirrels were acclimated in the behavioral room overnight. Animals were
594 weighed, transferred to clean cages, and allowed to habituate for 30 minutes. Squirrels were
595 immobilized with decapicones, injected with 2 mg/kg acylated rat ghrelin (1465, Tocris)
596 solubilized in PBS using an injection volume of 2 mL/kg body weight, and returned to their cages.
597 Control injections were PBS injected at a volume of 2 mL/kg body weight. Pre-weighed food was
598 added to the cage and animals allowed to feed for two hours. The food remaining after the
599 feeding period was weighed and used to calculate food consumption.

600 **Immunohistochemistry**

601 Ground squirrels were deeply anesthetized by isoflurane inhalation and then subjected
602 to intracardiac perfusion with PBS followed by fixative (4 % paraformaldehyde in PBS). Brains
603 were post-fixed overnight, and transferred to serial 10%, 20%, 30% sucrose solutions after
604 sinking. Brains were embedded in OCT, frozen on dry ice, and stored at -80 °C until use. Coronal
605 brain sections of the arcuate nucleus were cut at a thickness of 40 µm on a cryostat (Leica,
606 CM3050S). Sections were mounted onto SuperFrost Plus slides and stored at -80 °C with
607 desiccant until the day of the immunohistochemistry procedure. Sections were dried in an
608 incubator at 37 °C for 30 minutes. Slides were washed three times with PBS for 10 minutes, and
609 then washed with 1% H2O2 and 1% NaOH in PBS for 10 minutes. Slides were moved to 0.3%
610 glycine in PBS 1x for 10 minutes and washed with 0.03% SDS in PBS. Sections were blocked for
611 two hours at room temperature with 5% normal goat serum in 0.5% PBST.

612 For cFOS immunohistochemistry sections were incubated with primary antibody (1:500,
613 mouse monoclonal cFOS C-10, Santa Cruz, sc-271243) at 4 °C for 24 hours. After incubation with
614 the primary antibody, sections were washed four times with 0.1% PBST for 15 minutes. Sections
615 were incubated with secondary antibody (1:400, Alexa Fluor 488 goat anti-mouse, Invitrogen,
616 a11001) for two hours at room temperature. Sections were washed four times with 0.1% PBST
617 for 15 minutes, followed by a wash with PBS.

618 For pSTAT3 immunohistochemistry sections were incubated with primary antibody
619 (1:200, rabbit polyclonal Phospho-Stat3 (Tyr705), Cell Signaling Technology, 9131) at 4°C for 24
620 hours. After incubation with the primary antibody, sections were washed five times with 0.1 %
621 PBST for 10 minutes. Sections were incubated with secondary antibody (1:1000, Alexa Fluor 555
622 goat anti-rabbit, Abcam, ab150086) for two hours at room temperature. Sections were washed
623 five times with 0.1% PBST for 15 minutes, followed by a wash with PBS.

624 For POMC immunohistochemistry, sections were incubated with primary antibody
625 (1:2000, porcine anti-rabbit polyclonal POMC, Phoenix Pharmaceuticals, H-029-030) at 4°C for 24
626 hours. After incubation with the primary antibody, sections were washed five times with 0.1 %
627 PBST for 10 minutes. Sections were incubated with secondary antibody (1:1000, Alexa Fluor 555
628 goat anti-rabbit, Abcam, ab150086) for two hours at room temperature. Sections were washed
629 five times with 0.1% PBST for 15 minutes, followed by a wash with PBS.

630 Slides were mounted using Vectashield with DAPI. Sections were imaged on a Leica SP8
631 Confocal Microscope at 20X using the LASX software. Negative controls (secondary antibody

632 only) were performed for cFOS, pSTAT3, and POMC immunohistochemistry and showed no non-
633 specific fluorescent binding.

634 **Immuno-electron microscopy**

635 Ground squirrels were deeply anesthetized by isoflurane inhalation and were subjected
636 to intracardiac perfusion. Free-floating sections (50 µm thick) were incubated with rabbit anti-
637 AgRP antibody (Phoenix Pharmaceuticals) diluted 1:2000 in 0.1 M PB after 1 hour blocking in
638 0.1 M PB with 5% normal goat serum. After several washes with PB, sections were incubated in
639 the secondary antibody (biotinylated goat anti-rabbit IgG; 1:250 in PB; Vector Laboratories Inc.)
640 for two hours at room temperature, then rinsed several times in PB followed by incubation for
641 two hours at room temperature with avidin–biotin–peroxidase (ABC; 1:250 in PB; VECTASTAIN
642 Elite ABC kit PK6100, Vector Laboratories). The immunoreaction was visualized with 3,3-
643 diaminobenzidine (DAB). Sections were then osmicated (1% osmium tetroxide) for 30 minutes,
644 dehydrated through increasing ethanol concentrations (using 1% uranyl acetate in 70% ethanol
645 for 30 min), and flat-embedded in Durcupan between liquid release-coated slides (product no.
646 70880, Electron Microscopy Sciences). After embedding in Durcupan (14040, Electron
647 Microscopy Sciences), ultrathin sections were cut on a Leica Ultra-Microtome, collected on
648 Formvar-coated single-slot grids, and analyzed with a Tecnai 12 Biotwin electron microscope (FEI)
649 with an AMT XR-16 camera.

650 **Primary cell dissociation and single-cell RNA Sequencing.**

651 Primary neurons were isolated from the arcuate nucleus of hypothalamus and median
652 eminence following a published protocol[1] with modification. Animals were euthanized by
653 isoflurane inhalation overdose followed by cardiac perfusion with brain perfusion solution
654 (containing in mM: 196 sucrose, 2.5 KCl, 28 NaHCO3, 1.25 NaH2PO4, 7 Glucose, 1 Sodium
655 Ascorbate, 0.5 CaCl2, 7 MgCl2, 3 Sodium Pyruvate, oxygenated with 95% O2/5% CO2, osmolarity
656 adjusted to 300 mOsm with sucrose, pH adjusted to 7.4). The brain was dissected and slices were
657 cut on a vibratome (Leica, VT1200). A brain slice containing the ARC and ME were identified by
658 the presence of the third ventricle and separation of the optic chiasm. Three successive 600-µm
659 slices containing the ARC were collected. The area around the third ventricle was microdissected
660 from the brain slices using a micro-scalpel (Fine Science Tools, 10055-12).

661 Tissue was digested in Hibernate A medium (custom formulation with 50 mM glucose and
662 osmolarity adjusted to 280 mOsm, BrainBits) supplemented with 1 mM lactic acid (Sigma, L1750),
663 0.5 mM GlutaMAX (ThermoFisher, 35050061) and 2% B27 minus insulin (ThermoFisher,
664 A1895601) containing 20 U/ml papain (Worthington Biochemical Corporation, LS003124) in a
665 shaking water bath at 34°C for 30 min and dissociated by mechanical trituration through the tips
666 of glass Pasteur pipettes with decreasing diameter (0.9 mm, 0.7 mm, 0.5 mm, 0.3 mm). Cell
667 suspension was centrifuged over 8% bovine serum albumin (Sigma, A9418-5G) layer. Supernatant
668 was removed leaving ~50 µl of suspension. Cell suspension was resuspended in 950 µl of
669 Hibernate A medium (same formulation as above) and centrifuged at 300 rcf for 5 min.
670 Supernatant was removed, leaving ~50 µl of cell suspension, which was gently mixed with a glass

671 pipette and stored on ice. A 10 µl aliquot of cell suspension was mixed with 10 µl of Trypan Blue
672 stain, loaded into a hemocytometer, and used to assess cell concentration and viability.
673 Cell suspension was processed according to the 10X Genomics library preparation
674 protocol at the Center for Genome Analysis/Keck Biotechnology Resource Laboratory at Yale
675 University. Single cell suspension in RT Master Mix was loaded on the Single Cell G Chip and
676 partitioned with a pool of about 750,000 barcoded gel beads to form nanoliter-scale Gel Beads-
677 In-Emulsions (GEMs). The volume of cell suspension for loading was calculated based on cell
678 concentration to capture 10,000 cells. Upon dissolution of the Gel Beads in a GEM, the primers
679 were released and mixed with cell lysate and Master Mix. Incubation of the GEMs produced
680 barcoded, full-length cDNA from poly-adenylated mRNA. Silane magnetic beads were used to
681 remove leftover biochemical reagents and primers from the post GEM reaction mixture. Full-
682 length, barcoded cDNA was amplified by PCR to generate sufficient mass for library construction.
683 Enzymatic Fragmentation and Size Selection were used to optimize the cDNA amplicon size prior
684 to library construction. R1 (read 1 primer sequence) was added to the molecules during GEM
685 incubation. P5, P7, a sample index, and R2 (read 2 primer sequence) were added during library
686 construction via End Repair, A-tailing, Adaptor Ligation, and PCR. The final libraries contained the
687 P5 and P7 primers used in Illumina bridge amplification. Sequencing libraries were sequenced on
688 an Illumina NovaSeq instrument with 150 bp reads according to the manufacturer's instructions
689 at the depth of ~1.1-1.4 billion reads/sample.
690 Raw sequencing reads were processed using 10X CellRanger v.6.1.2 (10X Genomics,
691 Pleasanton, CA). Custom genome reference for thirteen-lined ground squirrel (*Ictidomys*
692 *tridecemlineatus*) was built based on the reference genome sequence and annotation obtained
693 from the Ensembl project (www.ensembl.org[2] Release 101; all files accessed on 11/20/2020):
694 Genome:
695 ftp://ftp.ensembl.org/pub/release-
696 101/fasta/ictidomys_tridecemlineatus/dna/Ictidomys_tridecemlineatus.SpeTri2.0.dna.toplevel.
697 fa.gz
698 Annotation:
699 ftp://ftp.ensembl.org/pub/release-
700 101/gtf/ictidomys_tridecemlineatus/Ictidomys_tridecemlineatus.SpeTri2.0.101.gtf.gz
701 The gene annotation was filtered to include only protein-coding genes using cellranger
702 mkgtf. 10X CellRanger was used to obtain transcript read counts for each cell barcode, filtered
703 for cell barcodes called as cells based on the default parameters. Read count matrix was further
704 processed using R 4.2.1, RStudio 2022.02.3, and Seurat 4.1.1[3]. Non-descriptive ground squirrel
705 gene symbols (i.e. those starting with "ENSSTOG…") were replaced with gene symbols of mouse
706 homolog genes, using the homolog conversion table from Ensembl. Initial set of cells/barcodes
707 was further filtered to include only those with >= 500 features/cells, >= UMIs/cells, and <= 10%
708 of mitochondrial genes (defined as those with gene symbol starting with "MT-"). This resulted in
709 ~11,000-20,000 cells/sample included in the dataset for further analysis, with the sequencing
710 depth of ~70-100k reads/cell. Read counts were processed according to the standard Seurat
711 analysis workflow, including normalization, identification of variable features, scaling, PCA,
712 clustering and visualization using UMAP plots. Graphs report normalized gene expression values.

713 ***De novo* Receptor Cloning**

714 Total RNA was isolated from the arcuate nuclei of active and IBA animals that had been
715 deeply anesthetized by isoflurane inhalation and subjected to intracardiac perfusion with ice cold
716 PBS. The brain was rapidly dissected and a vibratome (Leica VT1200) was used to cut 300-600 µm
717 coronal slices posterior to the separation of the optic chiasm. The area surrounding the third
718 ventricle, including the arcuate nucleus and median eminence, were manually dissected out from
719 the slices using 27 G needles and placed immediately into RNA lysis buffer from the Quick-RNA
720 Microprep Kit (Zymo, R1050). Total RNA was isolated from tissue using the Quick-RNA Microprep
721 Kit (Zymo, R1050). RNA concentration and integrity number (RIN) were assessed by an Agilent
722 2100 Bioanalyzer (Agilent, Santa Clara, CA). RNA concentrations were in the range of ~20 – 400
723 ng/µL and RIN values were in the range of 7.4 – 9.5. The resulting RNA was used for *de novo*
724 cloning of *Ghsr* and long-form *Lepr.* cDNA was prepared (Invitrogen SuperScript III First-Strand
725 Synthesus for RT-PCR, 18080-051) and the gene of interest amplified (Phusion High-Fidelity PCR
726 Kit, E0553S) using the following primers for *Ghsr:* forward 5'- CCAACTTGATCCAGGCTCC -3',
727 reverse 5'- CAAGTTCCGCTGTGCGATGG -3'; and *Lepr:* forward 5'- CAGGTACATGTCTCTGAAGTAAG
728 -3', reverse 5'- GCCACGTGATCCACTATAATAC -3'. Gel electrophoresis was used to isolate the
729 band of interest and DNA extracted using the Qiagen Gel Extraction Kit (28704). ORFs were then
730 ligated to topo vector (StrataClone Blunt PCR Cloning Kit, 240207). cDNA was sent for Sanger
731 Sequencing (Genewiz), and reference sequences compared the NCBI database.

732 **Hypothalamic Infusions**

733 Two hour and 24-hour food consumption were measured in paired IBA animals in two
734 separate experiments performed in the hibernaculum (4 °C, 40 – 60 % humidity, constant
735 darkness) across two different hibernation seasons (Winter 2021: hibernation season 1 and
736 Winter 2023: hibernation season 2) with two separate doses (15.3 nmol T3 for hibernation
737 season 1, 15.3 pmol T3 for hibernation season 2).For hibernation season 1, core body
738 temperature was measured by an abdominal implant, calibrated between 4 – 40 °C (EMKA
739 Technologies, M1-TA), and interscapular temperature was measured by an interscapular implant
740 (IPTT-300, BMDS). For hibernation season 2, only interscapular temperature (IPTT-300, BMDS)
741 was used to assess body temperature. Animals were implanted during the active season, while
742 they were euthermic, and allowed to recover for at least 2 weeks before implanted with
743 hypothalamic infusion cannulas as described below.

744 In a subsequent surgery, infusion cannulas (10 mm 26 G guide, 11 mm 33 G internal,
745 PlasticsOne) were implanted into the mediobasal hypothalamus during the active season while
746 animals were euthermic. Briefly, animals were induced into, and maintained at, a stable
747 anesthesia plane using isoflurane. Animals were administered 0.03 mg/kg preoperative
748 buprenorphine subcutaneously. The scalp was shaved and the animal transferred to a stereotax
749 (Kompf), where the skin was sterilized by repeated applications of betadine and 70% ethanol.
750 Sterile technique was used to expose the skull and drill a hole to allow for cannula implantation.
751 The following stereotaxic coordinates were utilized for cannula implantation: 0.5 mm posterior
752 bregma, 0.8 mm lateral midline, 8 mm ventral (guide cannula)/9 mm ventral (infusion cannula).
753 Two bone screws (2mm long, 1.2 x 0.25 mm thread, McMaster-Carr) and dental cement (RelyX
754 Unicem Resin, 3M, 56830) were used to anchor the guide cannula to the skull. A dummy cannula

755 was placed in the guide cannula until experiments were performed. Animals received a dose of
756 2mg/kg meloxicam in 1.5 mL saline subcutaneously immediately after surgery. Animals received
757 post-operative buprenorphine 0.03 mg/kg every 12 hours and meloxicam 1 mg/kg every 24 hours
758 intraperitoneally for 48 hours. Animals were allowed to recover for at least 2 weeks in pre-
759 hibernation environmental conditions in the vivarium (20 °C, *ad libitum* food and water, 40 – 60%
760 humidity, on Central Standard Time light-dark cycle) before they were brought to the
761 hibernaculum (4 °C, no food or water, 40 – 60 % humidity, constant darkness). Animals were
762 given three days to enter torpor (body temperature < 10 °C), after which they were monitored
763 for at least 1 week to ensure regular IBA:torpor bouts. Animals that failed to enter or maintain
764 hibernation during this time were excluded from the study and returned to the vivarium.
765 During hibernation season 1 (Winter 2021), feeding was first assessed at baseline (no
766 injection, during IBA 3 – 4). Animals were allowed to return to torpor after control experiments.
767 Hypothalamic T3 infusion (15.3 nmol per animal) was performed in the same animals after at
768 least 1 subsequent IBA had elapsed (corresponding to IBA 5 – 7).
769 During hibernation season 2 (Winter 2023), feeding was first assessed at after control
770 infusion (DMSO, during IBA 6 – 7). Animals were allowed to return to torpor after control
771 experiments. Hypothalamic T3 infusion (15.3 pmol per animal) was performed in the same
772 animals after at least 1 subsequent IBA had elapsed (corresponding to IBA 7 – 8), with the
773 exception of one animal which was tested on subsequent IBAs. For both hibernation seasons,
774 infusions were performed while animals were in the process of arousing from torpor. Animals
775 were identified as IBA candidates when abdominal temperature exceeded 8 °C and/or
776 interscapular temperature exceeded 10 °C. Squirrels were weighed and transferred to a clean
777 cage in the hibernaculum, kept at 4 °C in constant darkness. For infusions, when abdominal
778 temperature exceeded 16 °C and/or interscapular temperature exceeded 26°C, a connector
779 assembly consisting of PE50 tubing attached to an infusion cannula was loaded with control
780 DMSO vehicle or T3 (Sigma, T2877) solubilized in DMSO (Sigma, D2650). At this point, animals
781 were responsive to touch, but remained curled in the stereotypical torpor position and were
782 unable to move. Infusion solution was dispensed in a 1 µL bolus at a rate of 0.33 µL/min. The
783 infusion cannula was left in the guide cannula for two minutes to allow for the complete diffusion
784 of the infusion solution. The infusion cannula was removed and replaced with a dummy cannula.
785 For baseline (no infusion) experiments, animal body temperature was monitored until abdominal
786 temperature exceeded 16 °C and/or interscapular temperature exceeded 26 °C.
787 After infusion or baseline monitoring, animals continued to warm up. Once the abdominal
788 temperature surpassed 32 °C and/or the interscapular temperature surpassed 32 °C, animals
789 became mobile and explored their cages. Animals were allowed to habituate for 20 minutes. Dog
790 food was exclusively used for feeding consumption measurements. After habituation was
791 complete, a pre-weighed amount of food was placed in the cage. Animals were allowed to feed
792 for 2 hours, at which point the remaining food was removed, weighed, and returned to the cage.
793 Retrieving and weighing the food took less than 10 minutes per animal. The remaining food was
794 returned to the cage and the animal allowed to feed for a further 22 hours, to achieve a 24-hour
795 food consumption measurement.

796 **Hypothalamic Tissue Collection**

797 Naïve animals that had not undergone any experiment were euthanized by isoflurane
798 overdose and perfused with ice-cold PBS. The brain was removed from the skull and a ~6 mm
799 thick section collected from the optic chiasm to the mamillary bodies using a rat coronal brain
800 matrix (Electron Microscopy Sciences, 69083-C). The hypothalamus was isolated by removing
801 brain matter above the top of the third ventricle and lateral to the optic tract. Tissue was flash-
802 frozen in liquid nitrogen and stored at -80 °C until processing.

803 **Measurement of Hypothalamic T3**

804 Total triiodothyronine (T3) was extracted from frozen hypothalamus and purified as
805 reported previously[4]. Briefly, hypothalamic tissue was homogenized in 100% methanol
806 containing 1 mM 6-propyl-2-thiouracil (PTU) (Sigma, H34203) in a glass-glass tissue grind pestle
807 (60mm, Kontes, KT885300-0002). Homogenized tissue was centrifuged at 3000 rpm and
808 supernatant removed. The pellet was resuspended and washed twice more in 100% methanol
809 containing 1 mM PTU. T3 was extracted from supernatants and purified through solid-phase
810 chromatography using 200 – 400 anion exchange chloride resin (Bio-Rad, 140-1251) in Poly-Prep
811 chromatography columns (Bio-Rad, 731-1550). Columns were developed with 70% acetic acid
812 (Spectrum, AC110) and washed twice with water. Supernatants were passed through the column
813 without vacuum. T3 bound to columns was purified through a series of washes with acetate
814 buffer pH 7.0 and 100% ethanol. T3 was eluted with 2.5 mL 70% acetic acid. Extracts were
815 evaporated to dryness under nitrogen. T3 concentration was measured by ELISA (Leinco
816 Technologies, T181). Dried product was resolubilized in the zero-standard and the kit run
817 according to the manufacturer's instructions.

818 **Blood Brain Barrier Tracer Injections and Analysis**

819 Animals were anesthetized with isoflurane (4%) and injected in the tail artery with either
820 biocytin-TMR (ThermoFisher, T12921) or 3kDa dextran-TMR (ThermoFisher, D3307) at 10 mg/kg.
821 Animals were allowed to recover in their home cage for 30 minutes until perfusion fixation with
822 4% paraformaldehyde as described for Immunohistochemistry.

823 Brains were sectioned on a Leica cryostat at 40 mm and every tenth section was imaged
824 for blood brain barrier permeability analysis. Sections from dextran-injected animals were rinsed
825 with PBS and coverslipped with Vectashield containing DAPI (Vector Labs, H-1200). For biocytin-
826 injected animals, sections were immunostained to amplify fluorescence. After 1h block with 10%
827 bovine serum albumin (BSA) in PBS with 0.1% Triton-X-100, sections were incubated with
828 Streptavidin-AlexaFluor594 (1:1000 in 0.1% PBS-TritonX-100, ThermoFisher S11227) for 2h at RT.
829 Sections were washed three times with PBS, then coverslipped with Vectashield as above. Z-stack
830 images of liver and arcuate nucleus of the hypothalamus were acquired on a confocal microscope
831 (Zeiss, LSM-780) using ZEN Software. Maximum intensity projection images were used for
832 quantification in FIJI. Fluorescence intensity for the red channel was measured within circular
833 ROIs manually drawn over ARC-ME, or the entire field of view for liver. Brain tracer fluorescence
834 intensity was normalized to mean liver tracer fluorescence intensity from images with
835 standardized acquisition settings.

836 **Statistics, analysis, and data collection**

837 Statistical analyses were performed in GraphPad Prism v9.0 or higher (GraphPad
838 Software, San Diego, CA) for all comparisons with the exception of sc-sequencing analysis, which
839 was performed in R 4.2.1. Final figures were assembled in Adobe Illustrator. Data were tested for
840 normality using the Shapiro-Wilk normality test. When normality was assumed, the Student's t-
841 test was used to compare two groups, One-Way ANOVA was used to compare multiple groups
842 with one factor, and Two-Way ANOVA was used to compare multiple groups with two factors.
843 Dunnett's multiple comparison was used to find *post hoc* differences with one factor. Tukey's
844 multiple comparisons test was used to find *post hoc* differences among groups for Two-Way
845 ANOVAs. Paired data were analyzed with a paired Student's t-test. When data were not normal,
846 the Mann-Whitney test was used to compare two groups, and Two-Way ANOVA was used on
847 rank transformed data to compare multiple groups with two factors. Tukey's multiple
848 comparisons test was used to find *post hoc* differences among non-normal groups with two
849 factors. Sc-sequencing comparisons were performed using the Wilcoxin rank sum test.
850 Sample sizes and statistical data are reported in the text and figure legends. In the text, values
851 are provided as mean ± SEM, and $P < 0.05$ was considered statistically significant. No blinding
852 was used for behavioral data collection. Immunohistochemsitry quantification was performed
853 blinded. Individuals in experimental groups were chosen to best match body weight and to
854 represent both sexes across groups.